Application and Comparison of Different Control Techniques on Industrial Robotic Three Degree of Freedom (3DOF) Crane

Submitted by

MUHAMMAD FAISAL

MS

IN

ROBOTICS AND INTELLIGENT MACHINE ENGINEERING (RIME)

YEAR

2012

THESIS SUPERVISOR

DR MOHSIN JAMIL

SCHOOL OF MECHANICAL AND MANUFACTURING ENGINEERING

NATIONAL UNIVERSITY OF SCIENCES AND TECHNOLOGY

FORM TH-4

National University of Sciences & Technology

MASTER THESIS WORK

We hereby recommend that the dissertation prepared under our supervision by: (Student Name &Regn No.)______________________________________
Titled: ____be accepted in partial fulfillment of the requirements for the award of ____________________________________degree with (grade)

Examination Committee Members

1. Name:___________________________ Signature:________________

2. Name:___________________________ Signature:________________

3. Name:___________________________ Signature:________________

Co-Supervisor's name: ____________________ Signature:________________

Supervisor's name: ____________________ Signature:________________

Date:____________________

____
Head of Department

____
Date

COUNTERSINGED

Date:___________

____
Dean/Principal

DEDICATION

I thank to Allah Almighty the most gracious and the most beneficent for giving me everything in life. I dedicate this research work to my beloved family who support me in all crusts and troughs of life. I am also thankful to my supervisor who supported me to achieve this milestone.

I am extremely grateful to the National University of Sciences and Technology for funding this research project, which facilitated me to complete my Master degree.

A humble thanks to my colleagues and other people who helped me with their best capabilities.

DECLERATION

We hereby declare that no portion of the work referred to in this project Thesis has been submitted in support of an application for another degree or qualification of this of any other university or other institute of learning. In any act of plagiarism found, we are fully responsible for every disciplinary action taken against us depending upon the seriousness of the proven offence, even the cancellation of our degree

COPY RIGHT STATEMENT

AKNOWLEDGMENTS

It is the only Allah Almighty who is the source of every knowledge. Thanks Allah Almighty that gave me power and determination to complete this research project. A special thanks to my beloved parents and respected teachers that have been a permanent source of encouragement and motivation for me. I am also thankful to my colleagues that have supported me whenever I needed their help.

Abstract

A 3DOF crane is a lifting machine that mostly works with the use of pulleys and cables. For the construction and many other industries, cranes are valuable assets because they make working with heavy machinery and construction materials easy. These are widely used for moving, lifting and placing payloads from one location to another location. During the movement of payload, there is often an undesirable vibration or swing in the payload, and this payload vibration causes uneven trolley motion. So, for a smooth trajectory of a crane; a control technique, which gives a suitable input to the plant that causes a smooth trolley motion, is desirable.

In this research work, three control techniques namely PID tuned by LQR, PID tuned by pole placement and a dual loop control scheme has been investigated. The performance of three schemes has been analysed on controlling the trolley position and payload vibrational motion of the jib system of Quanser made three degrees of freedom (3DOF) crane. The classical PID techniques often face tuning issues. Issues such as overshoot, affect the smooth operation of crane if gains are not properly tuned. Many times large integral and derivative gains are required for smooth and safe operation of crane. That in practice is not feasible due to limitation of energy resources. In this research work, a dual-loop control scheme (DLCS) has been investigated to handle such type of issues. The DLCS, is a combination of classical PID and advanced state feedback control techniques. Extensive simulations have been carried out using MATLAB / Simulink and practically validated on a Quanser 3DOF crane prototype. The simulations and experimental results indicate that the proposed DLCS control scheme provides better results as compared to classical PID in context of overshoot and steady state error of the trolley position along with improvement of payload vibration.

Table of contents

List of Figures

List of Tables

List of Abbreviations

LQR	Linear Quadratic Regulator
3DOF	Three Degree of Freedom
PID	Proportional Derivative Integral
FLC	Fuzzy Logic Controller
DLCS	Dual Loop Control Scheme
DAQ	Data Acquisition Card
PC	Personal Computer
DC	Direct Current
LTI	Linear Time Invariant System

Chapter 1

Introduction

1.1 Introduction and background

The developments in the cranes have made things easy for humankind. These cranes are widely used in construction, shipment and industries [1-4]. The reason behind is that, without them lifting, delivering, and placing of heavy materials have to be done by human hands. That requires more time, have less efficiency and with more risk. A 3DOF crane [5, 6] usually consists of pulleys; that distribute the amount of force needed to lift a load, cable system; that is used to grip the payload, Levers; that directs the torque implicated and enable construction engineers to lift heavy loads easily. Winders, cables, ropes, chains and a basic level-pulley system are essential parts of any type of crane. The lever and other simple machines are helpful by decreasing the amount of force needed to carry out lifting and moving tasks. So, with the help of these components, it is mechanically more helpful to lift, shift and place heavy loads from one side to another side. There are many parameters that define the performance of crane operation. These parameters are time, force, stability and accuracy. Earlier cranes were manually operated. As the load or speed was increased to certain limits, it became difficult to handle cranes manually. It is due to fact that, 3DOF cranes have a serious problem of acceleration and deceleration, which causes to produce undesirable swing in the payload.

Therefore, the trend was to control the swing electronically using some control technique. The LQR controller has been applied to control the swing angle and position of payload [7]. However, the main problem with this technique was that it involves complex calculations. The system has fewer inputs than the degree of freedom that causes to complicate it. The fuzzy logic controller has also applied to control vibration of the 3DOF crane [8-10]. Fuzzy control has been introduced just to avoid the complex and time consuming calculations. The FLC has very simple structure and simpler practical implementation. Results of the FLC were improved as compared to LQR controller on the trolley vibration control [11]. Non-linear coupling control, improved the transient response of the crane [12].

The main issue with classical PID techniques is that it needs precise tuning[13]. It is often not possible to get desired output with minimum overshoot. Also, if we are interested to get reasonable tracking, we have to increase the integral and derivative gains to a large value. That requires more input energy expenditure, so, it is again not feasible. To improve the payload vibration and trolley issues we need some extension in classical PID control structure.

In this research work we have proposed a dual loop control scheme. It is a combination of classical PID and advance full state feedback techniques.

The paper is organized as follows. Chapter 1 explains the overall background of the study. Chapter 2 covers the literature review of the controllers that have been applied for controlling of the payload swing and the trolley position of 3DOF crane. Chapter 3 discusses the modeling of jib system of 3DOF crane. Chapter 4 presents the designing of classical PID control techniques. Our proposed dual loop scheme is discussed in Chapter 5. The simulation and experimental results are discussed in Chapter 6. The conclusion and future recommendations are briefed in chapter 7.

1.2 Thesis Objectives

Following points summarize the objective of our research work

- Study and address the payload vibration and trolley position of 3DOF crane.
- Study of anti-swing and position issues for open loop response of the system.
- Apply PID classical control techniques to control the anti-swing and position of crane.
- The tuning of classical PID controller by LQR algorithm.
- The tuning of classical PID controller by pole placement algorithm.
- To cater issues such as tuning and power consumption of classical PID techniques, an extension in main structure of PID has done. This, new control structure has named as dual loop control scheme (DLCS).

- A comprehensive simulations have been carried out on MATLA/Simulink to check the performance of three control schemes.
- Also, the performance of all three controllers has been experimentally validated on Quanser made 3DOF crane prototype.

1.3 Scope of Thesis

The development of suitable control technique for anti-swing and trolley position issues is an active area of research. It is an obvious thing because of the following applications of 3DOF crane.

- Actually, cranes are the backbone of construction industries. These are widely used in construction industries[14] for moving very heavy objects from one location to another location.
- In Integrated Circuits (IC) manufacturing industries, it is used to bring electrical components from one place to another place.
- Cranes are also used in rice mills to load and unload heavy packets of rice.
- These are also used in the car industry[15] for loading and unloading of the cars from one place to another.
- Cranes are widely used in electrical companies[16] for moving heavy objects like transformers from one location to another.
- Cranes are often used in steel mills[17] to carry heavy objects like steel rods from one position to another.
- Textile mills [18] also take some benefit of cranes for loading and unloading of textile goods.

It is also possible to extend this research work to other applications which involve automation for example,

- The controlling of artificial human hand motion.
- Smooth movement of automatic cars.

- Plane motion of belts that are controlled by motors for transportation of goods in shopping malls.
- The performance of electrical Elevators, which are often used in many buildings, can also be improved.

Research contributions of carried out research are listed as follows.

- M. Faisal, M. Jamil, U. Iqbal and Y. Ayaz, Selection of Suitable Control Techniques for Payload Anti-Swing and Trolley Position Problems of 3DOF Crane, 1st Applied Mechanical Engineering Conference AMEC-ETEX 2014, Lahore, 2014 **(Accepted).**
- Muhammad Faisal, Mohsin Jamil, Usman Rashid, Syed Omer Gilani, Yasar Ayaz, and Muhammad Nasir Khan, A Novel Dual-loop Control Scheme for Payload Anti-Swing and Trolley Position of Industrial Robotic 3DOF Crane, International Conference on Robotics ,Mechanics and Materials, Singapore, March, 2015 **(Accepted).**
- Muhammad Faisal, Mohsin Jamil, Qasim Awais, Usman Rashid, Muhammad Sami, Syed Omer Gilani , Yasar Ayaz and Muhammad Nasir Khan, Iterative Linear Quadratic Regulator (ILQR) Controller for Trolley Position Control of Quanser 3DOF Crane, International Conference on Green Computing and Engineering Technology (ICGCET 2015), Dubai, 2015 **(Accepted).**

1.4 System Description

The Quanser 3DOF crane is shown in Figure 1. It is a compact version of a tower crane. Similar to actual crane, it has three degrees of freedom. It has three parts, namely tower, jib and payload. A general block diagram of 3DOF tower crane is given in Figure 2. Discussion of each part is given in coming sections.

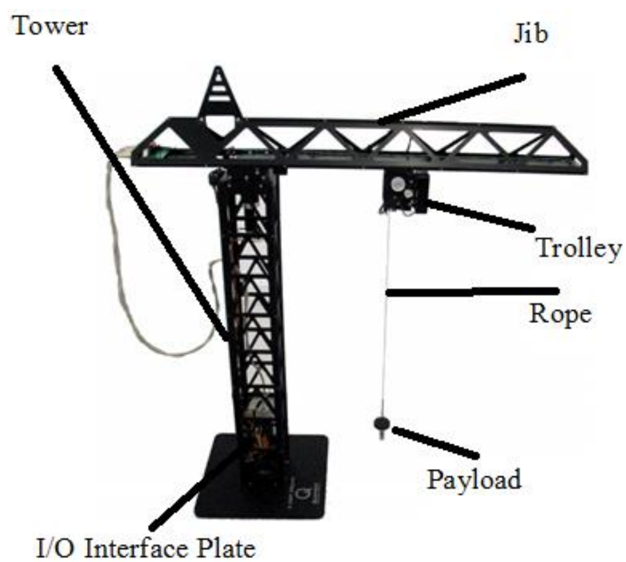

Figure 1(a): The Quanser three degrees of freedom (3DOF) crane prototype

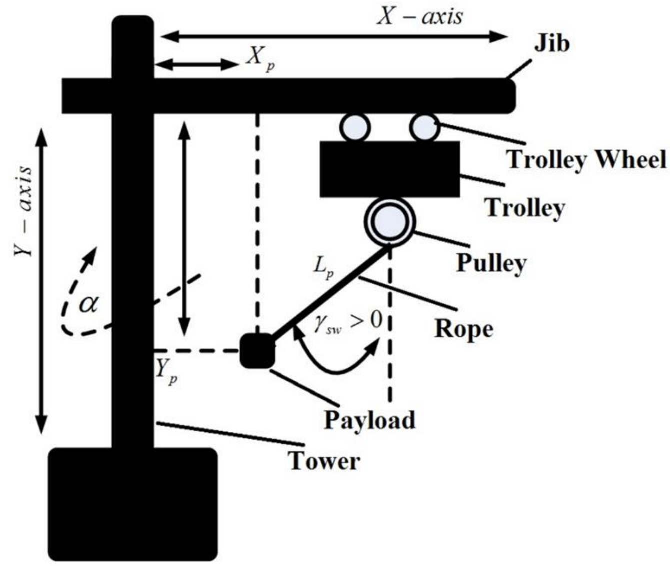

Figure 2(b): Block diagram of 3DOF crane

1.4.1 Tower System

Figure 3 shows the block diagram of the crane tower (also known as mast). It holds the bulk of this system's structure while also containing an electrical input/output circuit board near its base. This circuit interfaces with a Q8 terminal board to allow sensor signals and motor actuator signals to travel back and forth between the crane and a PC. The horizontal member, mounted atop the tower, can rotate clockwise and counterclockwise by using a motor for actuations.

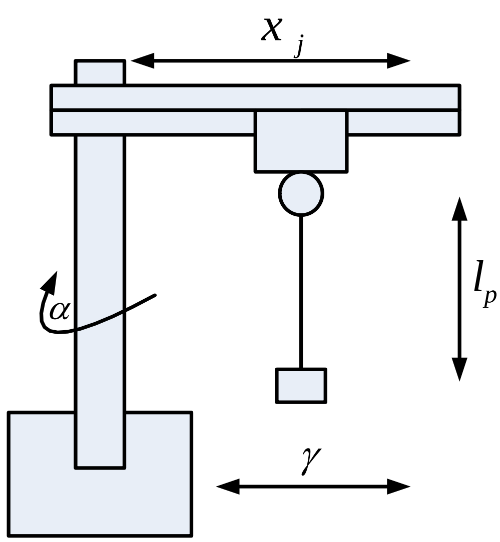

Figure 3: General block diagram of 3DOF crane

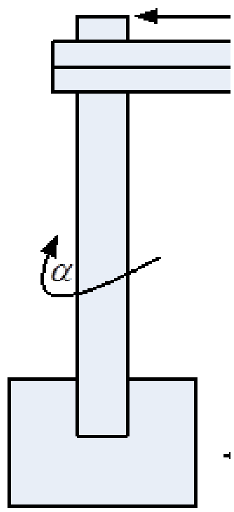

Figure 4: Tower system of 3DOF crane

1.4.2 Jib System

The horizontal member is called the jib or boom of the crane. Figure 4 shows the jib system of 3DOF crane. This jib has a trolley that can move back and forth on a linear track. The maximum distance that is allowed to cover by trolley of jib system is 0.4 meters. There are limit switches placed in extreme positions of jib system for trolley protection. Whenever, the trolley touches the limit switches, simulation stops and trolley halt its motion. It retains its position until we reset the limit switches.

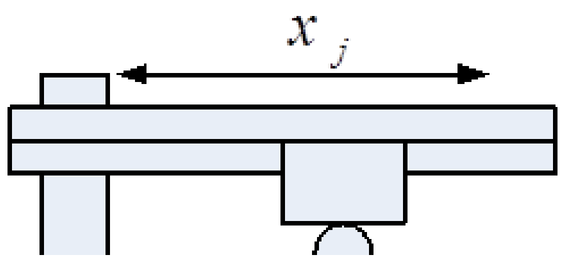

Figure 5: Jib system of 3DOF crane

1.4.3 Payload system

The jib has a trolley that has a cable to lift to the payload up or to set it down directions by using another motor for actuation. Each of the motorized shafts are instrumented with optical encoders.

The motors are driven by linear current control amplifiers with the capability of 100 watts each. A limit switch has been mounted on the maximum allowed distance of payload in upward direction. Whenever, the payload touches the limit switch, simulation stops and trolley halt its motion. It retains its position until we reset the limit switch. Figure 5 shows the payload system of 3DOF crane. The Quanser 3DOF crane prototype is often used to teach the fundamentals of the control of the tower cranes, as well as advanced topics such as efficient and reasonable fast load transportation that simultaneously employs load swing minimization.

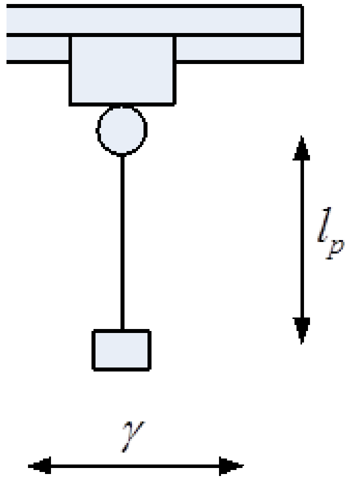

Figure 6: Payload system of 3DOF crane

1.4.4 AMPAQ Power Module

The AMPAQ power module is shown in Figure 6. It is actually a pulse-width modulated[19] current amplifier. The motors of 3DOF crane are driven by AMPAQ power module unit. The signal from the data-acquisition board are to be connected to the input connector of the AMPAQ. The sense connector outputs the current measured in the attached DC motor.

Figure 7: AMPAQ Power Module

The Enable connected socket of the AMPAQ receives digital input signals from the PC in order to enable or disable the power modules. Finally, the amplified current is sent from the output connector of AMPAQ power module to crane motors.

1.4.5 Input / Output interface plate (I/O plate)

The I/O plate is shown in Figure 7. It is attached near the base of the crane's tower and has connector sockets that allow to the 3DOF crane to interface directly with the Quanser Q8 hardware-in-the-loop terminal board and a Quanser AMPAQ Power Module

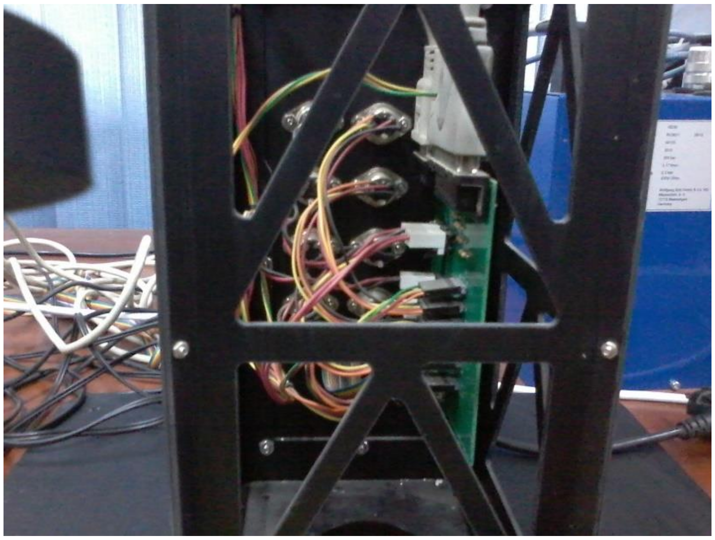

Figure 8: Input/ Output interface plate

1.4.6 Data Acquisition Card

The data acquisition card is used to get the information signal from the decoder and limit switches from Input/ Output plate of 3DOF crane. And then after comparison with desire input, gives an error signal to the AMPAQ Power Module. So that, it provides a reasonable input to motors of 3DOF for reference tracking. Figure 8 shows the diagram of data acquisition card.

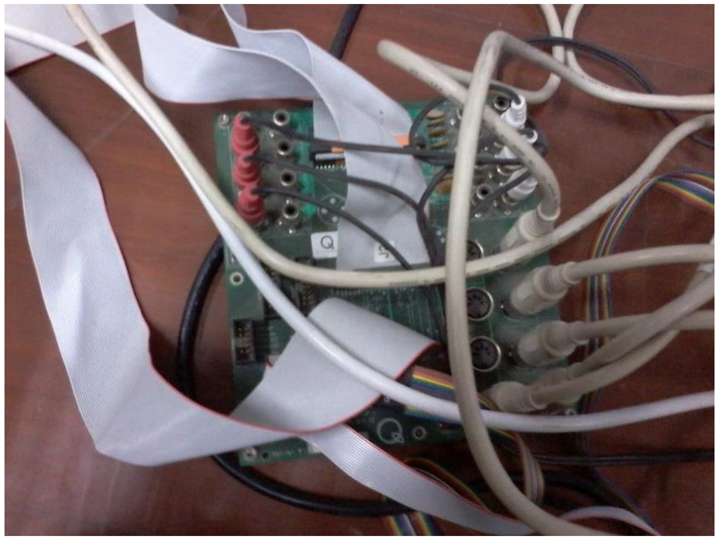

Figure 9: Data Acquisition Card

1.4.7 Connection between 3DOF crane, AMPAQ and data-acquisition board

Simplified block diagram of the connections between 3DOF crane, the AMPAQ Power Module and the data-acquisition card is provided in the Figure 9. A number of encoders are placed on different locations of the 3DOF crane. The data from encoders is sent to the Data Acquisition Card Terminal Board through I/O interface plate placed on the 3DOF crane. The computer, after receiving the data from the Data Acquisition Card Terminal Board, send signal to AMPAQ Power Module to drive the motors for achieving the set points.

The Enable signal is provided by the computer to the AMPAQ Power Module. It is used to inform to the AMPAQ Power Module that either it should **ON** the power module or not.

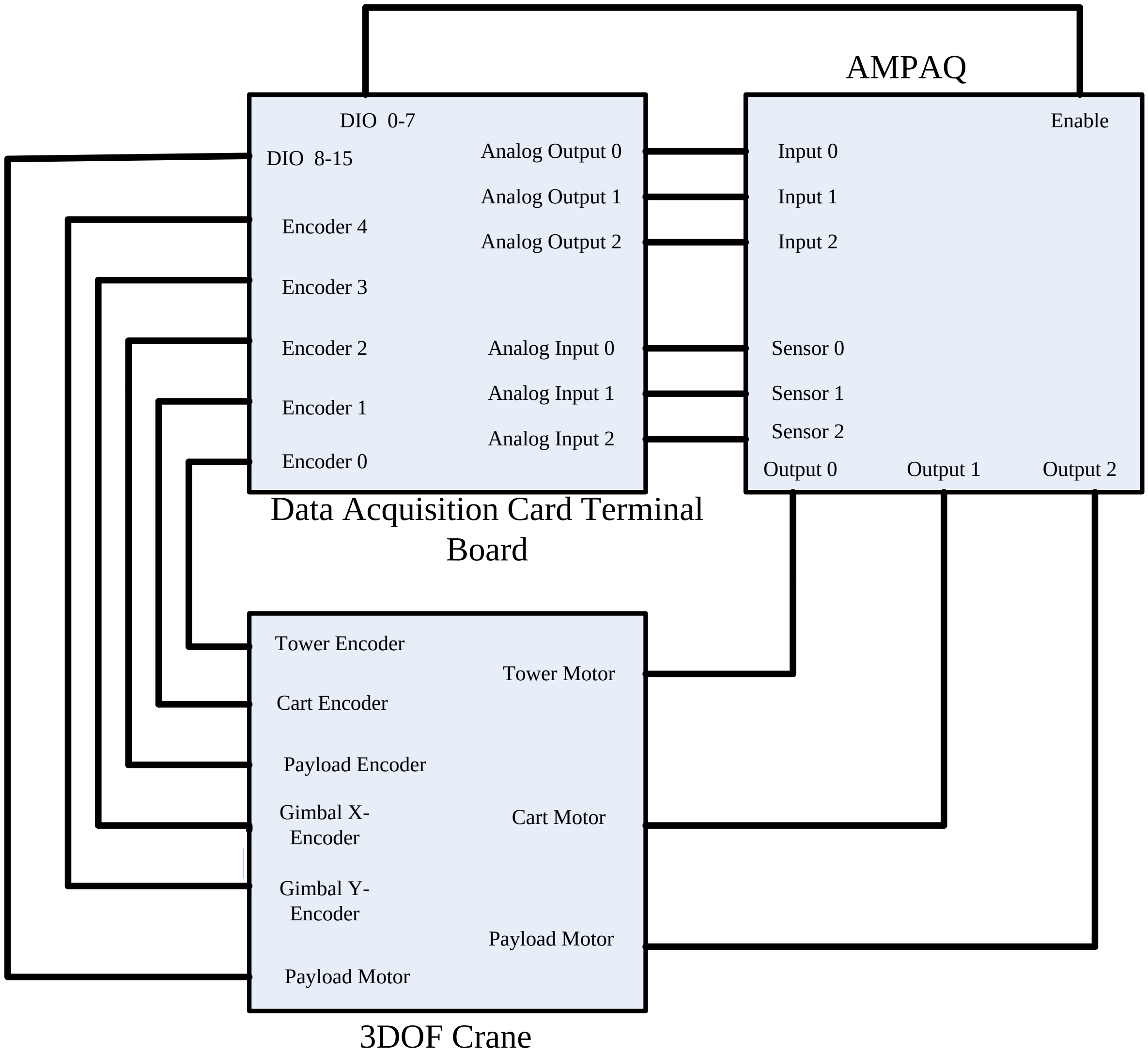

Figure 10: Block diagram of connection between 3DOF crane, Data Acquisition Card and AMPAQ

Chapter 2

Literary Review

A number of researchers have devoted their valuable time for payload anti-swing and trolley position control of the jib system of 3DOF crane. The main focus has been upon the minimization of transportation time keeping in account the performance measures, including overshoot, settling time and steady state error. To minimize the oscillations of payload, the combination of position servo control and fuzzy logic control is a very effective technique [20]. The idea of intelligent controller like fuzzy controller can be extended to the optimal controller for damping the vibrations [21]. The selection of suitable control technique as required by the operation of 3DOF has been discussed in [22]. Another researcher work is about the investigation of the non-linear coupling law. It involves adaptive and non-adaptive schemes using Lyapunov-based stability for the asymptotic tracking of the crane position along with improvement of payload swing [23].

A non-linear controller supported by partial feedback implementation technique is very efficient in the presence of varying pendulum length [24]. A comprehensive review on 3DOF cranes is presented in [25]. In another research work, a payload has been treated as a summation of tiny masses, But in this approach twisting of the payload about rope is another performance measure in addition to payload swing and trolley position [26]. Lyapunov function can be used for confirmation of stability of the plant, if there exists an algorithm of switching of control signal values on the surface where system behavior is independent to parameter variation [27]. Using Lyapunov function along with sliding-surface control, the behavior of plant with varying initial conditions is discussed in [28].

The behavior of a crane is investigated with a time varying parameter, namely length of rope, with the supposition of ignoring the payload weight as compared to trolley weight [29]. To track the desired trajectory by a slow system, a singular perturbation time-scale separation can be used instead of control input to stabilize the vibration [30]. Investigation of the swing angle with varying payload is another interesting approach [31]. The oscillations of any tall structure object in presence of any external force like air or earthquake shocks can be controlled using active mass damper [32].

Vibrations can also be controlled by motion planning schemes like minimum time trajectory planning which may include parameters like bounded velocity, swing, acceleration and jerks of the trolley[33].

To minimize the steady state error keeping in account the transient response, PID with neural compensation is a very fruitful approach [34]. Genetic optimizing techniques have used for a good performance under a range of operating conditions with reduction of vibration during the positioning of the payload cart [35]. In the context of Fuzzy, Fuzzy PD-based control is very efficient in the reduction of operating time to the improvement of payload swing [36]. A very efficient approach to minimize the vibration of payload is by changing the accelerating directions as contrary of decelerating the trolley during the operation [37]. Integral sliding mode with disturbance observer is another approach to control the payload swing [38].

Motion planning algorithm relying on kinematics problem is another scheme for handling position and swing problems [39]. Combination of feed forward input shaping method with classical control theory results in a very useful control approach to regulate the position and stabilization of swing [40, 41]. Another researcher's work is about the tele-operation control for liquid container transportation by an overhead crane structure that permits the machinist to handle the speed of the overhead crane easily and to feel the swing of the rod mechanically through the response force [42].

The neural network technique is very helpful for vibration control because it involves learning capability [43-46]. The individual limitations or draw backs of neural networks and fuzzy logic are effectively solved by using them together in form of neuro-fuzzy [47-50].

Chapter 3

Modeling of System

3.1 Modeling of jib system

The Quanser 3DOF crane is very helpful hardware in the loop for the testing of controllers which can lately be applied on actual industrial 3DOF crane for practical purposes. Basic information is given, detail can be seen on Quanser 3DOF user manual [51]. It has three controllers, separately for jib, tower and payload. Payload can move up and down. Downward distance is considered positive. A maximum vertical distance of payload from jib arm is 0.8636 m. Jib trolley can move linearly on linear guide. Towards the end point (opposite to tower) velocity is considered as positive. A maximum distance of the trolley from the pivot is 0.8065m.

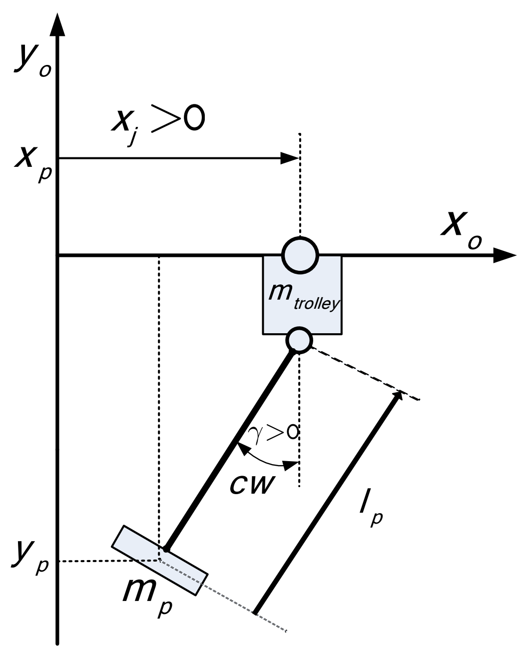

Figure 11: Free Body Diagram of Jib System

The maximum rotation of jib about tower axis is 360 degrees. So, it is 3DOF hardware. To avoid from serious damage on extreme conditions, few safety switches and limit switches are also included in package. Small description of jib modeling is discussed here. The jib system is represented as two-dimensional linear gantry by supposing that payload is suspended at a certain height with a steel cable.

It is also assumed that cable remains rigid. The payload can move along jib axis similar to an inverting pendulum [52] as in Figure 10. Ideally, this angle of the suspended payload along the jib axis (often know as a swing angle) should be zero. But practically it has some value, varying from 0 to a maximum limit, depending upon the acceleration and deceleration of the trolley.

3.2 State space of 3DOF crane

Here the linear state-space representation of the 3DOF crane jib is included. Actually, the system is nonlinear; the Lagrange technique [53, 54] is used to get the dynamics of the jib system. The nonlinear system of equations are linearized and represented in the state-space format.

Linear representation of the state-space of the 3DOF crane jib system is:

$$\frac{\partial}{\partial t} x_J = A_J x_J + B_J u_i \tag{1}$$

$$y_J = C_J x + D_J u_i \tag{2}$$

Here, A_J , B_J , C_J and D_J are system matrices. x_J , represents system's states matrix. u_i , is the input to the plant. The system states are given below:

$$x_J^T = [x_j(\mathrm{t}), \gamma(\mathrm{t}), \frac{d}{dt} x_j(\mathrm{t}), \frac{d}{dt} \gamma(\mathrm{t})] \tag{3}$$

Representing from left to right: position of trolley, swing angle of payload along jib axis, the velocity of the trolley and rate of swing angle.

And system matrices are below:

$$A_J = \begin{bmatrix} 0 & 0 & 1 & 0 \\ 0 & 0 & 0 & 1 \\ 0 & -\dfrac{m_{payload} r_{j\_pulley}^2 g_{griv}}{m_{trolley} r_{j\_pulley}^2 + J_{E\_\psi} K_{g\_j}^2} & 0 & 0 \\ 0 & -\dfrac{g_{griv}(m_{trolley} r_{j\_pulley}^2 + m_{payload} r_{j\_pulley}^2 + J_{E\_\psi} K_{g\_j}^2)}{m_{trolley} r_{j\_pulley}^2 + J_{E\_\psi} K_{g\_j}^2} & 0 & 0 \end{bmatrix} \tag{4}$$

$$B_J = \begin{bmatrix} 0 \\ 0 \\ \dfrac{r_{j\_pulley} \eta_{g\_j} K_{g\_j} \eta_{m\_j} K_{t\_j}}{m_{trolley} r_{j\_pulley}^2 + J_{E\_\psi} K_{g\_j}^2} \\ \dfrac{r_{j\_pulley} \eta_{g\_j} K_{g\_j} \eta_{m\_j} K_{t\_j}}{(m_{trolley} r_{j\_pulley}^2 + J_{E\_\psi} K_{g\_j}^2) l_{h\_p}} \end{bmatrix} \tag{5}$$

$$C_J = \begin{bmatrix} 1 & 0 & 0 & 0 \\ 0 & 1 & 0 & 0 \end{bmatrix} \tag{6}$$

$$D_J = \begin{bmatrix} 0 \\ 0 \end{bmatrix} \tag{7}$$

From above system matrices we may identify that our system is a single input multi output (SIMO). Input is current and outputs are the position of trolley and swing angle of payload. Putting the values of variables, given in Appendix A, in the matrices A_J and B_J we have achieved following matrices.

$$A_J = \begin{bmatrix} 0 & 0 & 1 & 0 \\ 0 & 0 & 0 & 1 \\ 0 & -1.7019 & 0 & 0 \\ 0 & -13.3301 & 0 & 0 \end{bmatrix} \tag{8}$$

$$B_J = \begin{bmatrix} 0 \\ 0 \\ 18.2478 \\ 21.12 \end{bmatrix} \tag{9}$$

Chapter 4

PID Controller Design

4.1 Overview of jib controller

The dimension of the system matrix A_J is 4×4. If we use it directly without any change in dimension during the calculation of gains using any method etc. LQR or pole placement. Then we get PD controller. For the sake of implementation of the PID controller, we have added one column in the start and one row in the last of the matrix A_J, keeping all new entries zero except the entry $A_J(5,1)$ which is kept 1. It is just because of the reason that we want more focus on the position of the trolley. So, the purpose of 5th gain, namely integral gain is that it is responsible for smooth trajectory of jib trolley.

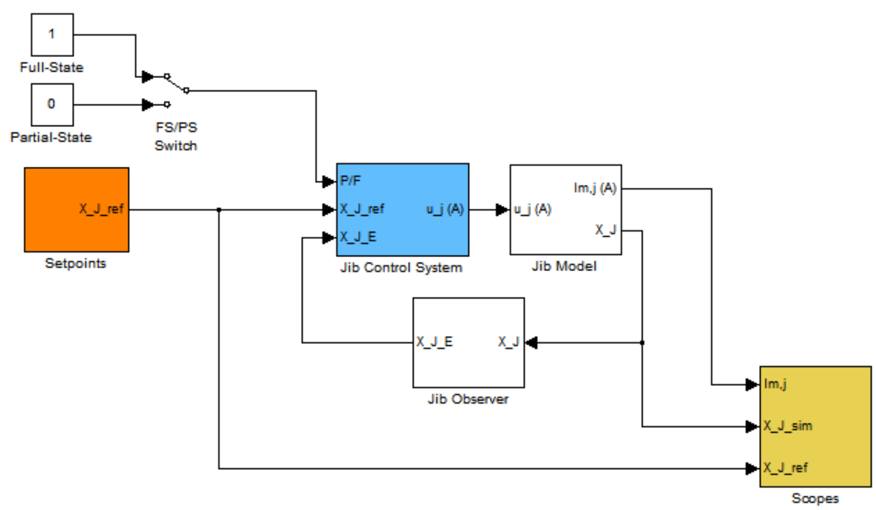

Figure 12: Simulink model of jib controller

We have two measurable output states namely position and swing angle. Increase of speed of the trolley can cause an increase in payload swing. An increase in swing angle not only disturbs the

3DOF crane function, but in extreme cases may damage the structure of hardware. So, we need some mechanism to find the controlled force that helps in smoothen the trolley trajectory with reduction of payload vibration, keeping in mind the speed, time and safety as performance measures. Figure 11 shows the Simulink model of the 3DOF crane jib controller. Figure 12 shows the block diagram of jib controller.

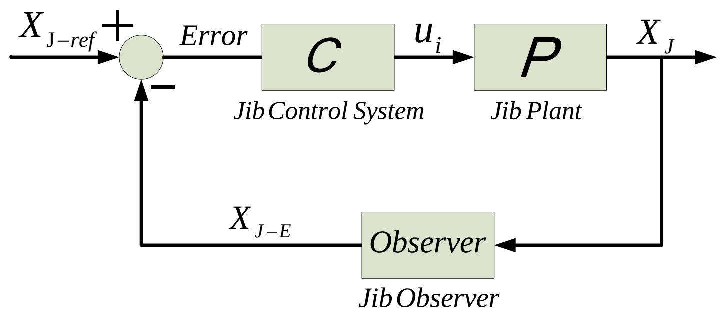

Figure 13: Block diagram of jib controller

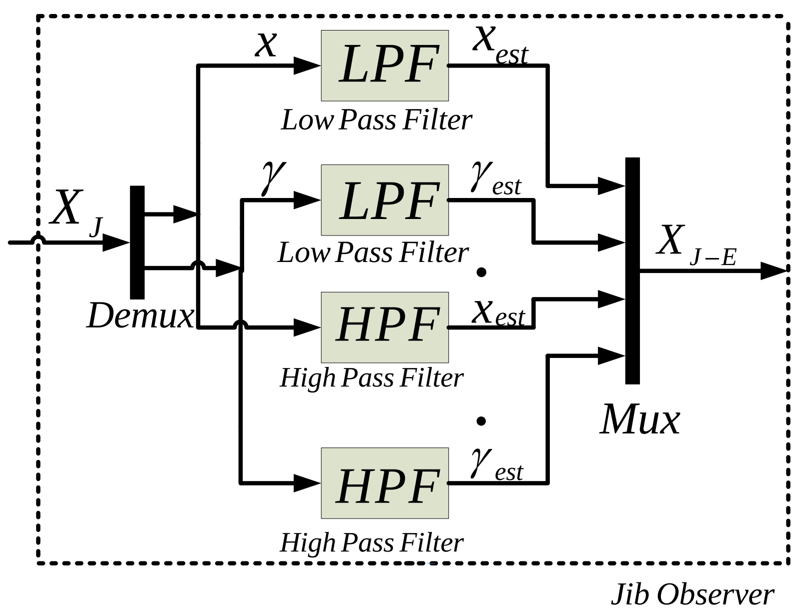

Figure 14: Block diagram of jib observer

Here, as we know that we have only two measureable states namely position and swing, so, there is need of some observer arrangement that helps to feedback all four states instead of two states. Here, the observer is nothing but an arrangement of low pass and high pass filters as shown in Figure 13.

The jib control system consists of PID gains. The tuning of PID has done either by LQR or by pole placement methods. These methods will be discussed in coming sections. The jib control system consists of five gains. First four are PD gains and remaining is integral gain. Figure 14 shows that block diagram of the jib control system.

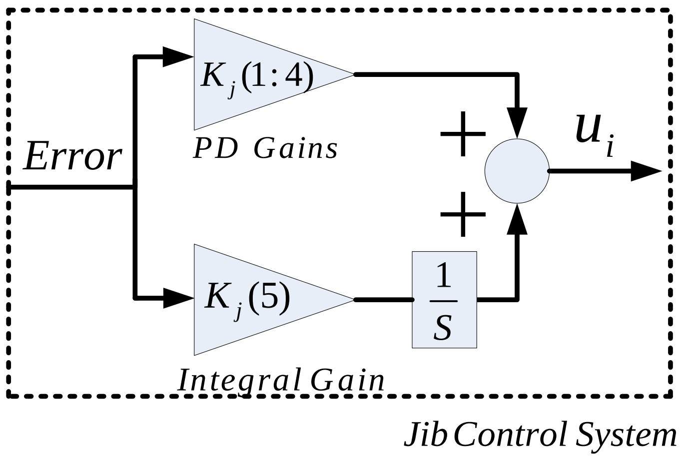

Figure 15: Block diagram of the jib control system

The jib plant is represented in Figure 15. Here, the actuator dynamics bound the input that is to be supplied to the plant. The closed loop overview of the jib system can be visualized in Figure 16.

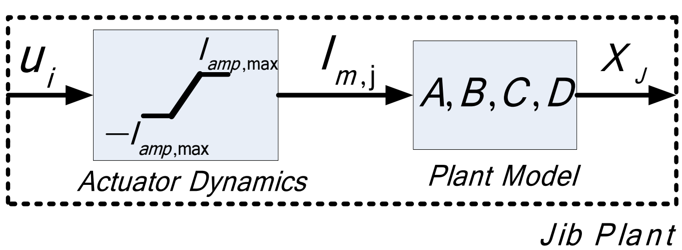

Figure 16: Plant model with actuator dynamics

4.2 LQR tuned PID

PID gains are calculated by LQR. Firstly, we have discussed the qualitative features of state space representation of the system. Main two ideas known as controllability and observability [55] of the system. The controllability and observability are distinctive features of state-space investigation. The E. G. Gilbert and R. F. Kalman are pioneers of these outstanding ideas. They gave a comprehensible clarification that cancellations of unstable poles are unwanted even if complete cancellation is possible. Brief description of controllability is given below and observability of the same system will be discussed in the next chapter.

For the system having state space:

$$\dot{x} = Ax + Bu \tag{8}$$

$$y = Cx + Du \tag{9}$$

Here, $A \in R^{nxn}, \mathrm{B} \in R^{nxr}, \mathrm{C} \in R^{mxn}, \mathrm{D} \in R^{mxr}$ are plant matrices. The controllability of system is discussed here.

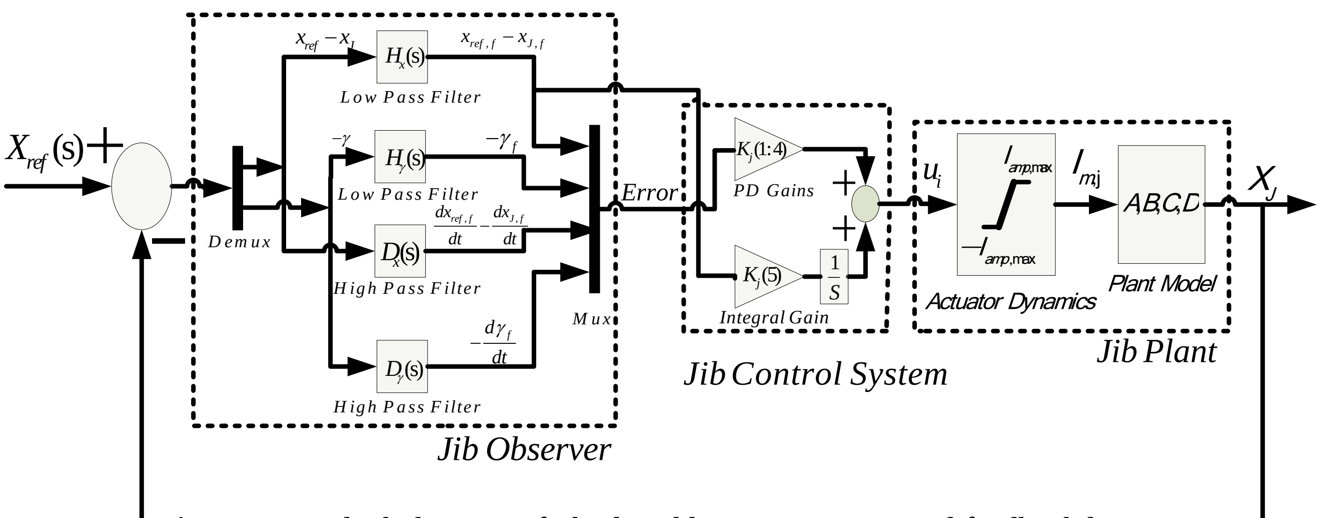

Figure 17: Block diagram of jib-closed loop position control feedback loop

4.2.1 Controllability

A linear time-invariant plant[56], as discussed in Equation 8 and Equation 9 or by the pair (A, B), is said to be controllable if there is an existence of an input, u(t) ,where $0 \le t \le t_b$, that force system from any initial state $x(0) = x_a$ to any other state $x(t_b) = x_b$ in a limited time t_b . In converse, the system described in Equation 8 and Equation 9 or (A, B) is said to be uncontrollable.

4.2.2 Controllability Grammiam

The n-dimensional linear time-invariant plant as discussed in Equation 8 and Equation 9 or the pair (A, B) is said to be controllable if and only if any of the subsequent comparable states is satisfied:

1) The controllability grammiam

$$w(0,t_l) = \int_0^{t_l} e^{A\tau} BB^T e^{A^T\tau} d\tau = \int_0^{t_l} e^{A(t_l-\tau)} BB^T e^{A^T(t_l-\tau)} d\tau \tag{10}$$

is none singular for all $t_l > 0$.

2) The $n \times nr$ controllability matrix $U = \begin{bmatrix} B & AB & A^2B & \ldots\ldots & A^{n-1}B \end{bmatrix}$ is full rank
3) The $n \times (n+r)$ matrix $\begin{bmatrix} A - \lambda_A I & B \end{bmatrix}$ has full row rank at each Eigen value λ_A of A .

So, keeping in mind the above definition of controllability, we verified our system in accordance to definition defined in the second step and our system is controllable.

4.2.3 Linear Quadratic Regulator (LQR) Algorithm

In accordance to plant defined in Equation 8 and Equation 9, In LQR [57] our aim is to carry initial states which are not zero, to zero best possibly. This is the direction oriented problem. The function (cost function) carries the linear quadratic form as:

$$J_c = \int_0^\infty (x^T Qx + u_i^T Ru_i)dt \tag{11}$$

As J_c is scalar, so we can easily prove that weighting matrices, Q and R are symmetric, intuitively $Q^T = Q$ and $R^T = R$. Where Q and R appear normally in diagonal. Besides, here it is also a supposition that Q is semi-positive definite:

$$Q = \begin{bmatrix} q_1 & 0 & \dots & 0 \\ 0 & q_2 & \dots & 0 \\ \dots & 0 & \dots & \dots \\ 0 & \dots & \dots & q_n \end{bmatrix}, q_i \geq 0, i = 1, 2, \dots, \mathrm{n} \tag{12}$$

Similarly, R is positive definite:

$$R = \begin{bmatrix} r_1 & 0 & \dots & 0 \\ 0 & r_2 & \dots & 0 \\ \dots & 0 & \dots & \dots \\ 0 & \dots & \dots & q_n \end{bmatrix}, r_i \geq 0, i = 1, 2, \dots, \mathrm{m} \tag{13}$$

The control law that minimize the J_c heads towards the linear state feedback:

$$u_i = -K_c x \tag{14}$$

Here K_c is a constant matrix with the condition of A, B, C, Q, R are also constant matrices. One key point that can easily be derived that weighting matrix Q relates to states x and R relates to u_i. Intuitively, if we concern more to input, then we increase value of weighting matrix R. And if output is more important parameter than we increase weighting matrix Q. Here K_c, can be found by

$$K_c = R^{-1}B^T P \tag{15}$$

Keeping in mind K_c, the closed loop system is

$$\dot{x} = (A - BK_c)x \tag{16}$$

Here one assumption is that with K_c, plant is stable. Now, assume P is $n \times n$ symmetric matrix that is satisfying the following Algebraic Riccati Equation (ARE) [58].

$$A^T P + PA + Q = PBR^{-1}B^T P \tag{17}$$

So, finally, optimal control law is:

$$u_i = -R^{-1}B^T Px \tag{18}$$

PID gains are calculated by the above mentioned LQR method by the following weight matrices.

$$R = 0.1;$$
$$Q = \begin{bmatrix} 5 & 0 & 0 & 0 & 0 \\ 0 & 5 & 0 & 0 & 0 \\ 0 & 0 & 1 & 0 & 0 \\ 0 & 0 & 0 & 5 & 0 \\ 0 & 0 & 0 & 0 & 1 \end{bmatrix} \tag{19}$$

These are actual weighting matrices that implied in the 3DOF crane system. In next sections a number of control techniques are used to find the controlling force for the same 3DOF crane system and detail comparison is also done.

With the help of Figure 16 it can be observed that actual control law takes the form of:

$$u_i = -K_c \zeta^T_{j\_e} \tag{20}$$

Here, value of $\zeta^T_{j\_e}$ is:

$$\zeta^T_{j\_e} = \left\{ \begin{array}{l} x_{j\_f}(t) - x_{j\_df}(t), \gamma_f(t), \\ \left(\frac{d}{dt} x_{j\_f}(t) - \frac{d}{dt} x_{j\_df}(t) \right), \\ \frac{d}{dt} \gamma_f(t), \int \left(x_{j\_f}(t) - x_{j\_df}(t) \right) dt \end{array} \right\} \tag{21}$$

Where, $\zeta^T_{j\_e}$ is estimated error state that includes $x_{j\_df}(t)$ and $x_{j\_f}(t)$ which are filtered reference position of trolley and filtered measured position of the trolley. That are passed through a low pass filter $H_x(\text{s})$. $\frac{d}{dt} x_{j\_f}(t)$ is the velocity of trolley after being processed through a high pass filter $D_x(\text{s})$. $\frac{d}{dt} x_{j\_df}(t)$ is filtered velocity set point which infect a calculated trajectory that is only passed through a low pass filter. Similarly, $\gamma_f(t)$ and $\frac{d}{dt}\gamma_f(t)$ are filtered swing angle and filtered velocity of the swing angle after being processed through low pass and high pass filters respectively. General steps involve in LQR algorithm are given in Figure 17.

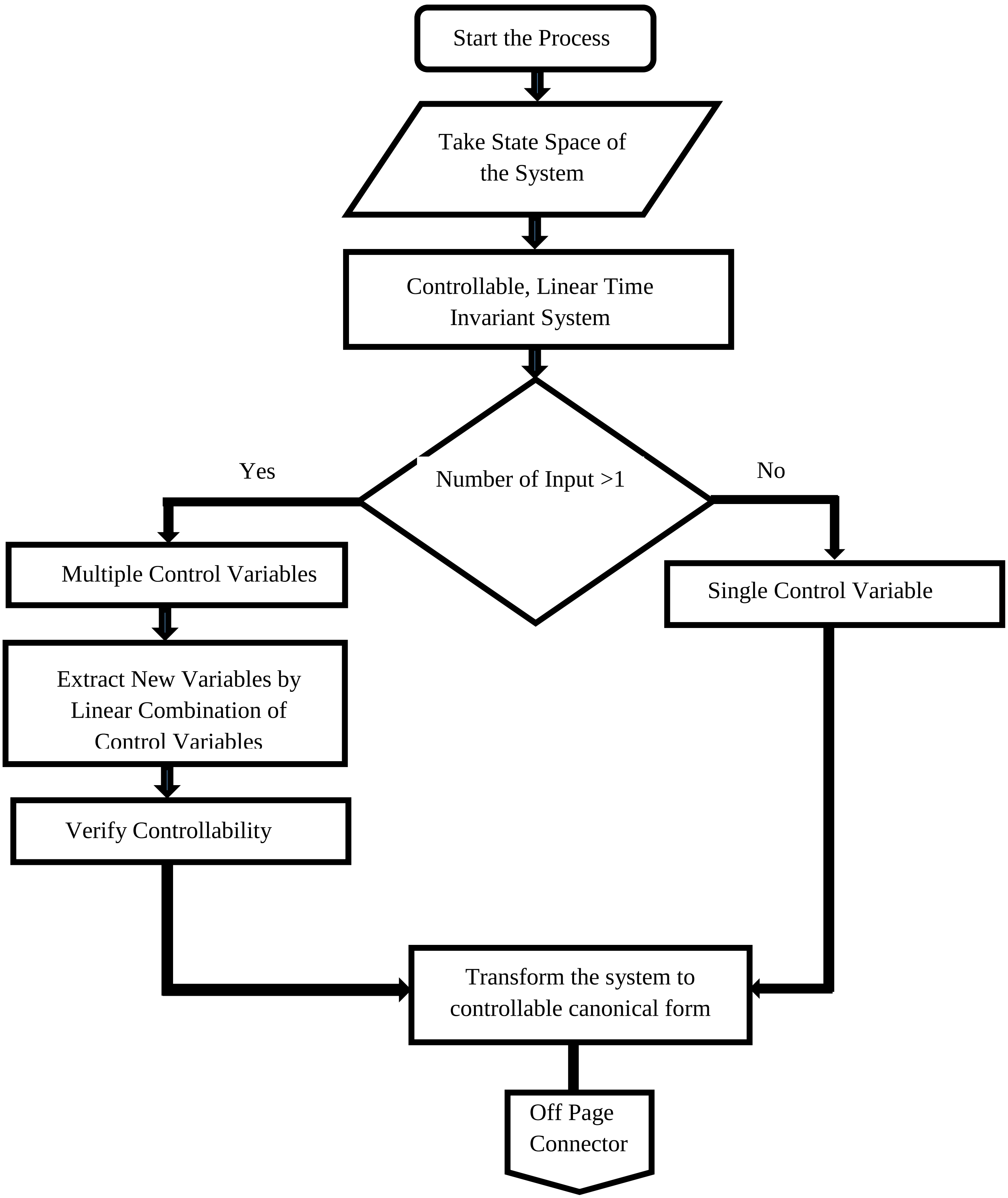
Start the Process
Take State Space of the System
Controllable, Linear Time Invariant System
Number of Input >1
Yes
No
Multiple Control Variables
Single Control Variable
Extract New Variables by Linear Combination of Control Variables
Verify Controllability
Transform the system to controllable canonical form
Off Page Connector

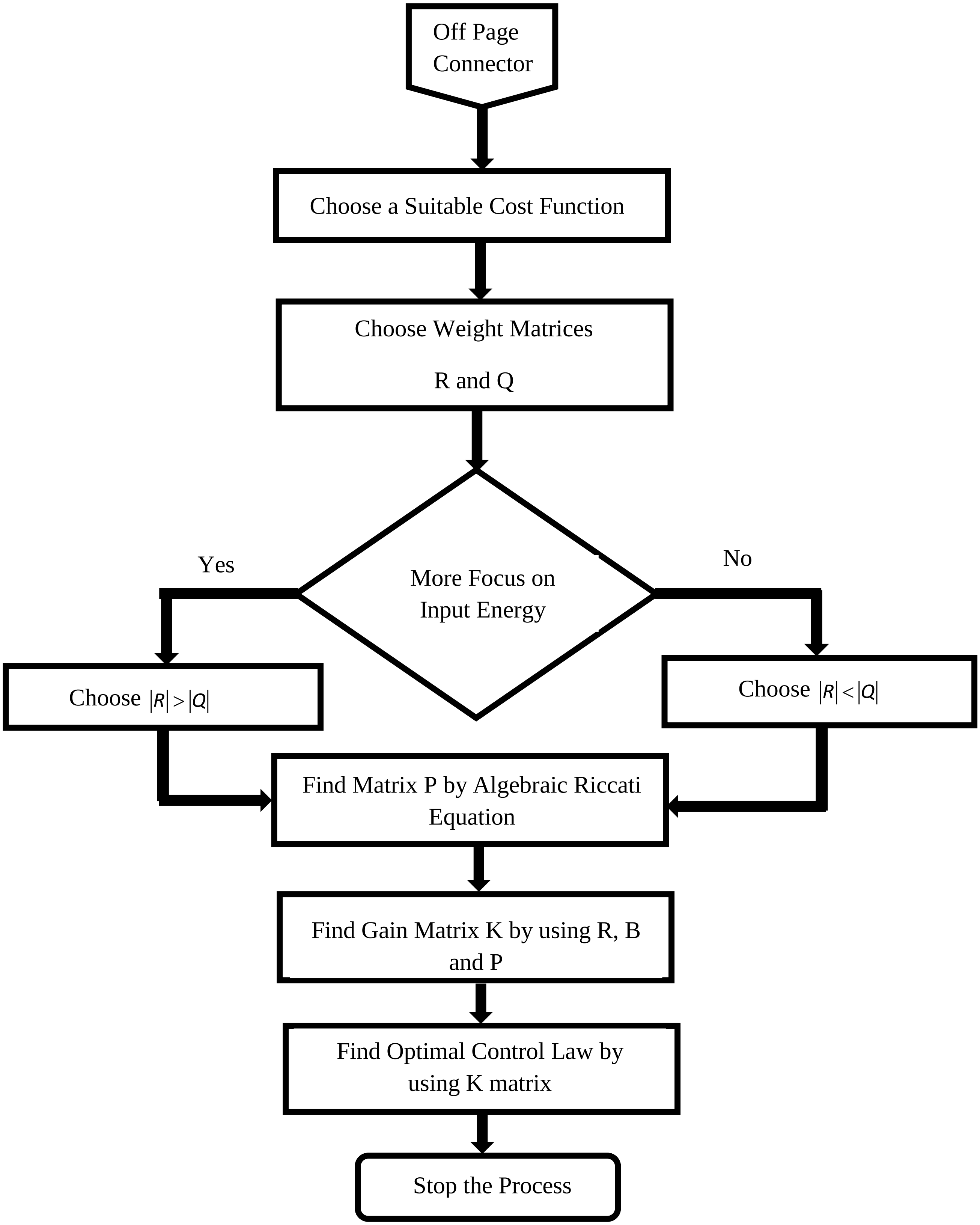

Figure 18: Flow chart of LQR algorithm

4.3 Pole Placement tuned PID

State feedback [59] is advance technique that can be used to improve performance and robustness of the system. A number of methods can be used for this purpose, namely pole placement, optimal control, decoupling [60]and servo control [61]. Here we will discuss only the pole placement algorithm. Time dependent specification of plant mostly involves certain requirements which strongly relate to time response of the system. For example, when the step response of the stable plant is under consideration, we express system output with parameters like rise time, settling time and overshoot. In pole placement techniques [62]. We usually place poles, 3 to 5 times faster than the system poles. So, after making the poles faster, system response varies significantly. With this algorithm we can adjust the rise time, settling time and overshoot according to our need. This implies that pole locations find out stability and performance of the plant.

In this paper, we placed the poles by Ackermann formula because it involves only one inverse. Ackermann formula is:

$$K_c^T = \left[0, \quad 0, \quad ....., \quad 0, \quad 1\right] C^{-1} \phi_d(A) \tag{22}$$

Where, C, is controllability matrix, discussed in previous section. And the characteristic polynomial $\phi_d(A)$ for the desired poles is.

$$\phi_d(A) = \phi_d(\mathrm{s})|_{s=A} = A^n + \gamma_{n-1}A^{n-1} + ... + \gamma_o I_n \tag{23}$$

Also, $A^0 = I_n$, using this method we placed our desired poles at

$$P = \left[-1-1i \quad -1+1i \quad -3+10.1i \quad -3-10.1i \quad -2\right] \tag{24}$$

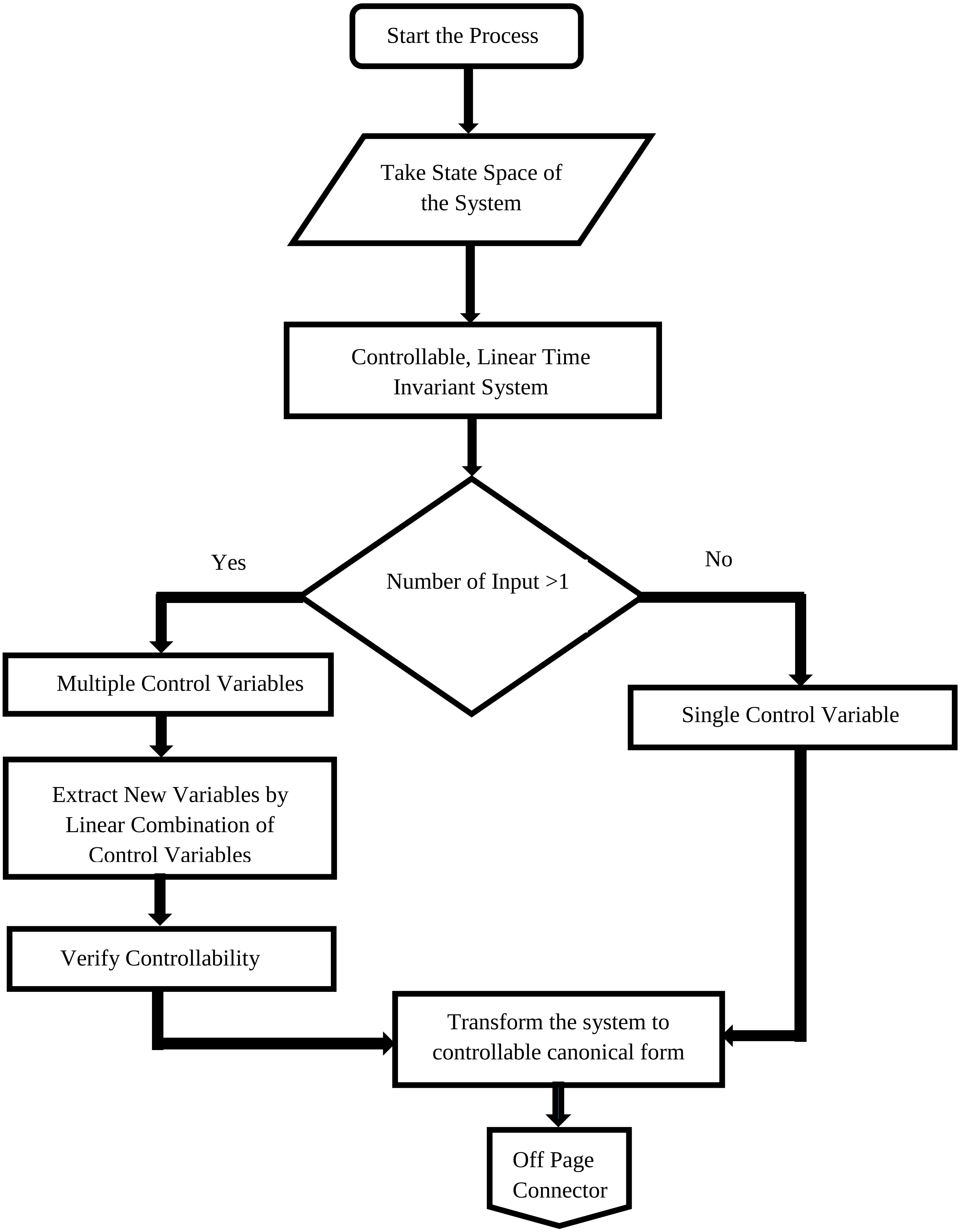
Start the Process
Take State Space of the System
Controllable, Linear Time Invariant System
Number of Input >1
Yes
No
Multiple Control Variables
Single Control Variable
Extract New Variables by Linear Combination of Control Variables
Verify Controllability
Transform the system to controllable canonical form
Off Page Connector

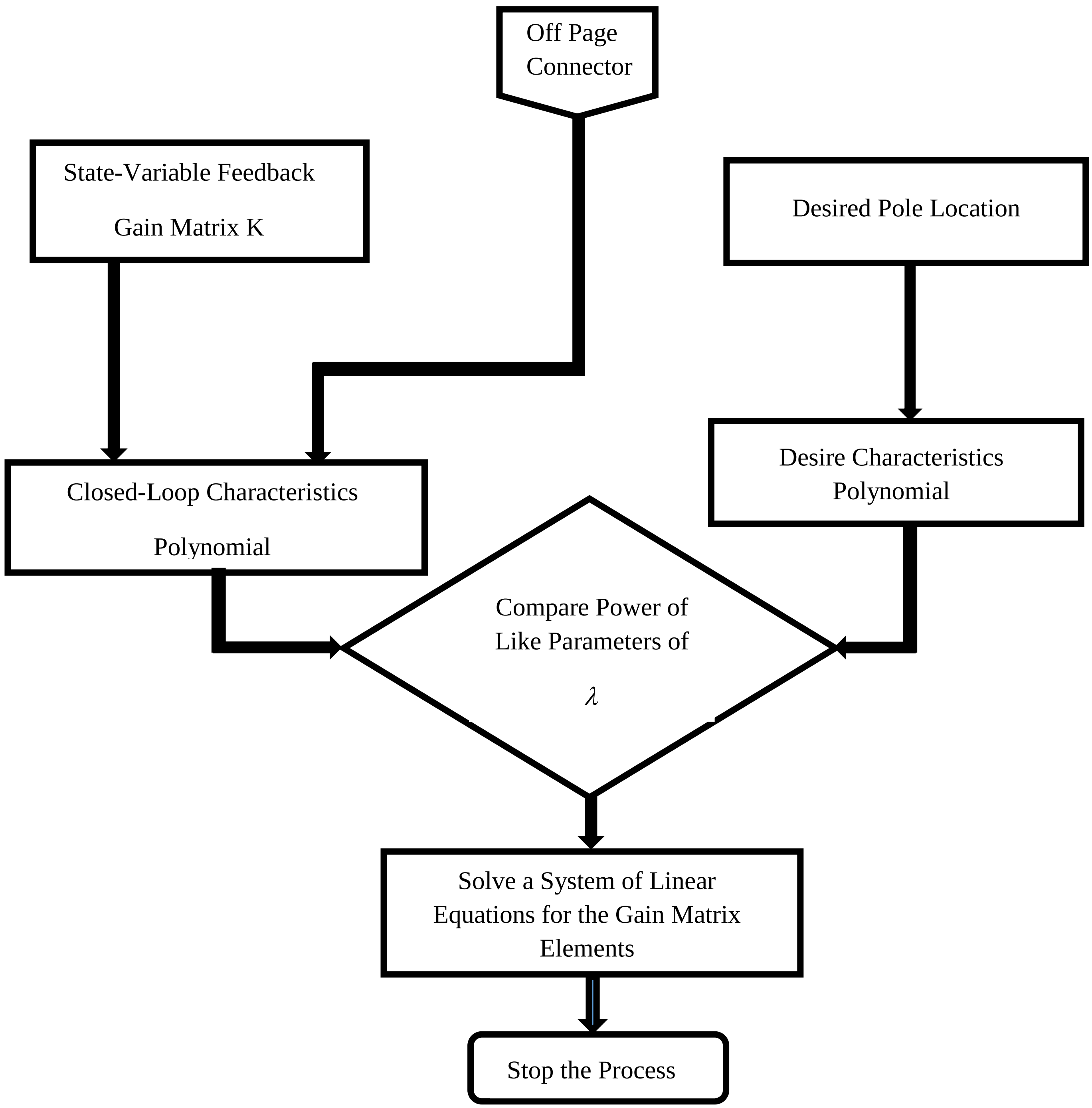

Figure 19: Flow chart of pole placement algorithm

This gives gain matrix with five gains. PID by LQR gains are replaced by PID by pole placement in the Simulink model as in Figure 11. General steps involve in pole placement algorithm are given in Figure 18.

Chapter 5

Proposed Dual-Loop Control Scheme

5.1 Observability

A very closely related theory to controllability is observability of the plant. The main key point about controllability and observability is that controllability helps in navigation of states with the help of input, whereas observability assists in estimation of states with help of output. So, in observability we see the effects of all states on the output. The observability is defined as:

A linear time-invariant (LTI) plant is observable if every unidentified initial state $x(0)$ can be found by knowing the input $u(\mathrm{t})$ and the observation of output $y(\mathrm{t})$ over a finite time period. If not, the LTI plant is unobservable. The study of observability of the plant is generally done on an unforced plant.

5.2 Observability Grammiam

The n-dimensional linear time-invariant system as presented in Equation 8 and Equation 9 or the pair (A, C) is observable if and only if the $n \times n$ matrix given below is non-singular for $t > 0$

$$M(0,t) = \int_0^t e^{A^T \tau} C^T C e^{A\tau} d\tau \tag{25}$$

5.3 Observer Design

There are many limitations of state feedback, for example, all state variables are not directly measurable, also sensitivity to uncertainties. So we need some algorithm to estimate [63] the states which are not directly accessible. For that, we have designed an observer that helps to estimate full states even fewer states are not directly assessable. Secondly, we may design robust control like H-infinity controller [64] or H-2 [65] controller. That may be part of future work. Intuitively, the state space approach uses state feedback is:

$$u_i = -K_c x + Fr \tag{26}$$

Where K_c is the gain (or gain matrix in case of multiple states), and F is feed forward, in most cases no feedforward is used. So it is kept zero, so control law becomes

$$u_i = -K_c x \tag{27}$$

But usually, x (all state variables) is not accessible, only partial y (output) is measurable. To implement state feedback without knowing all system states $x(t)$, it is necessary to use state estimation. Block diagram of full state feedback is given in Figure 19.

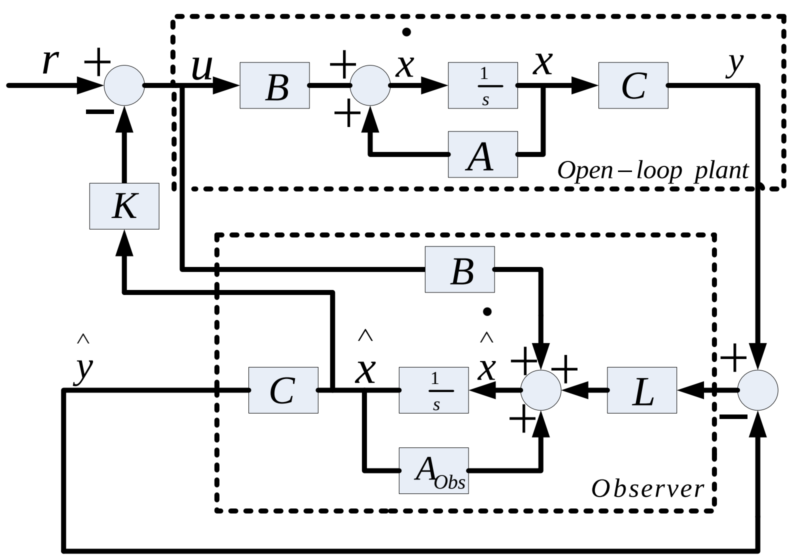

Figure 20: Block diagram of full state feedback

Simple equation of state estimator of jib controller is given below.

$$\dot{\hat{x}} = A_{obs}\hat{x}_e + Bu_i + L_g e_r \tag{28}$$

Here, $B_J = B$ is system input matrix. e_r , is the error between measured outputs and estimated outputs. That has found by the following relation:

$$e_r = y - \hat{y} \tag{29}$$

And the estimated output is

$$\hat{y} = C\hat{x}_e \tag{30}$$

$C_J = C$ is system output matrix. The observer state matrix A_{obs} is obtained through the relation:

$$A_{obs} = A_J - L_g C_J \tag{31}$$

Here, L_g is an observer gain matrix which in our paper is found by the pole placement method discussed in the previous section. The only difference is that here we use matrix C instead of B matrix. $\hat{x}_e$, is estimated states vector, $\hat{y}$ is estimated output. A_{obs} is an observer state matrix, B_J, C_J are original system matrices .

Desired poles are placed at:

$$P = 5*[-1-1i \quad -1+1i \quad -3+10.1i \quad -3-10.1i] \tag{32}$$

Simulink model of the observer designed for full state feedback is shown in Figure 20.

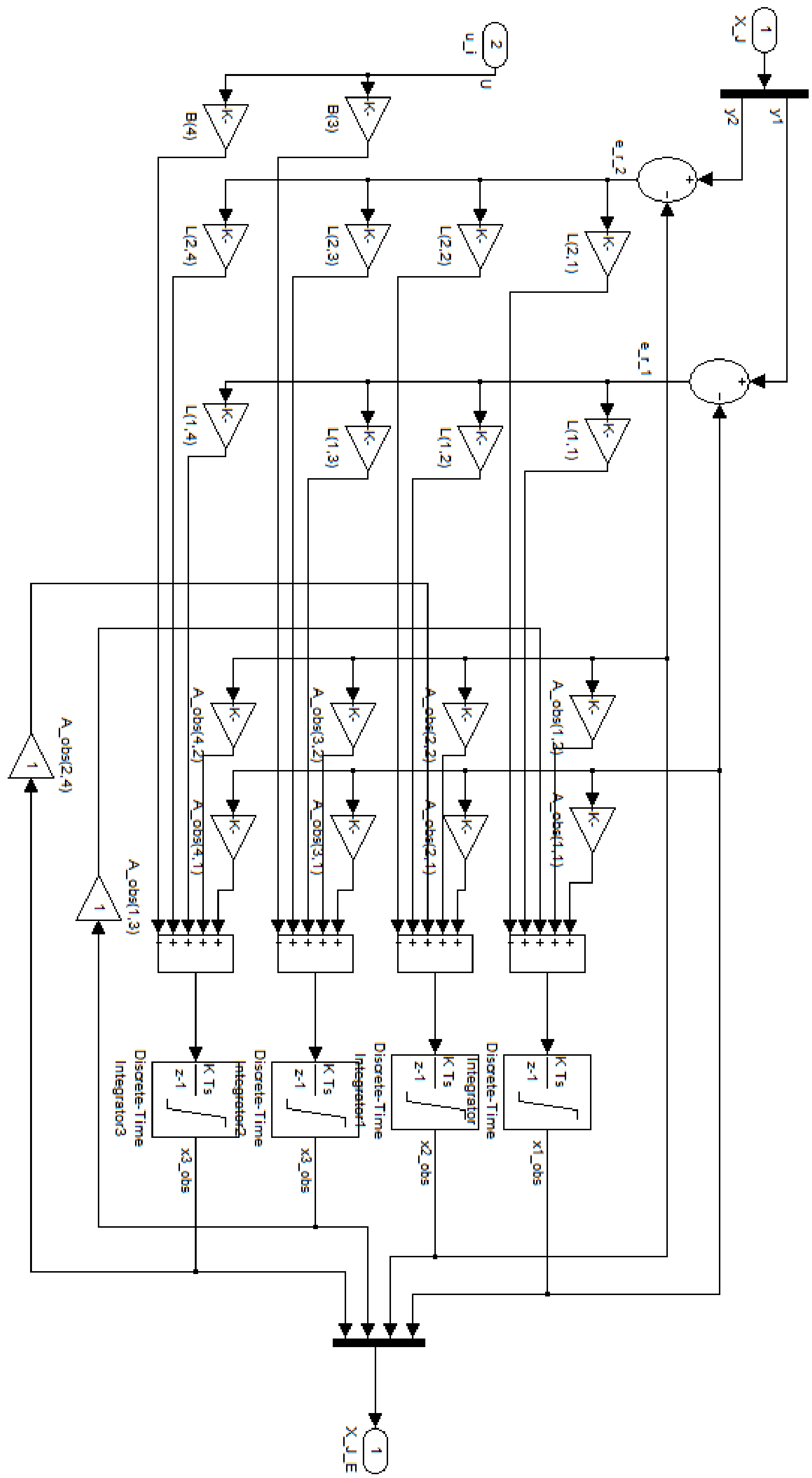

Figure 21: Simulink model of observer

5.4 Full State Feedback

As the limitations of state feedback, due to partial states measurement, is amazingly solved by the observer design that helps in estimation of all states even in the presence of partial states. Now, we can easily design full state feedback [66] with the help of estimated states. By using state feedback law while ignoring feed forward and placing measurable states with estimator states we have control law:

$$u_i = -K \hat{x}_e \tag{33}$$

Where K is found using LQR. Here we have selected input weights as given below:

$$R = 1$$
$$Q = \begin{bmatrix} 1 & 0 & 0 & 0 \\ 0 & 1 & 0 & 0 \\ 0 & 0 & 1 & 0 \\ 0 & 0 & 0 & 1 \end{bmatrix} \tag{34}$$

So, finally, u_i is input that will be provided to plant.

5.5 Proposed Dual Loop Control Scheme

In classical PID technique, a big problem that mostly arises is overshoot. So, for that we have developed a dual-loop control scheme (DLCS) which is a combination of classical PID and advance full state feedback control techniques. Figure 21 shows the concept of our proposed structure of DLCS controller.

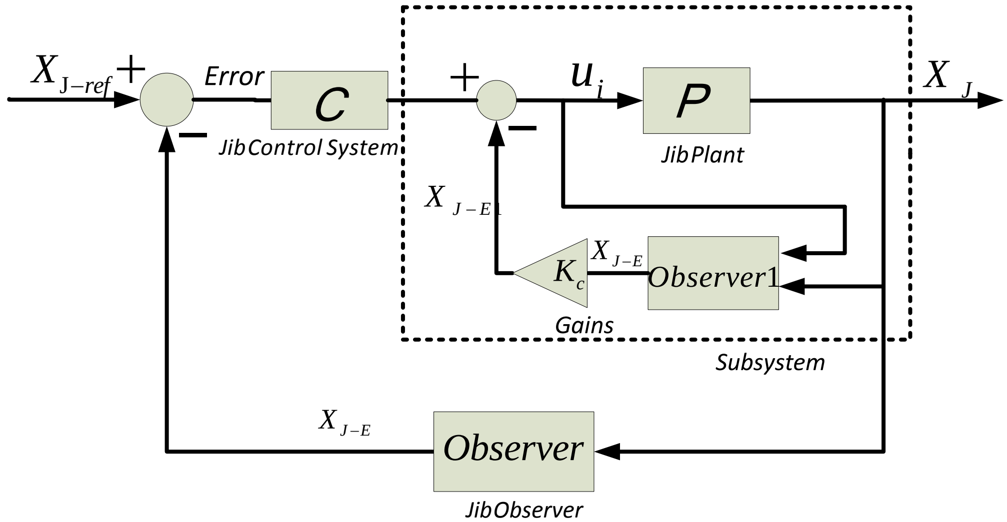

Figure 22: Block diagram of dual loop control scheme for jib system

Here, the internal fast part relates to full state feedback and outer slow part is feedback to PID. The output swing and position are feedback to internal and external comparators. Now if you review the previous section where we have developed a full state feedback for jib system. You can observe that we choose very fast poles for the observer design. So, that will work in simulation of jib system. But practically do not work because of limitations of the hardware. That's why, we have included this full state feedback structure in the subsystem instead of replacing the actual control structure. Figure 22 shows the Simulink model of the proposed structure.

The advantage of this algorithm is very fruitful. The justification is that when we choose fast poles, the system response was very fast. So, when we feedback to the reference, hardware did not work due to its limitation. Then, when we accompanied it in subsystem, response in subsystem became faster. So, response of states became faster. Now, when the improved response feedback to the main loop, it provided better results. Along with the improvement in the overshoot, settling time, steady state error with reduction of payload vibration.

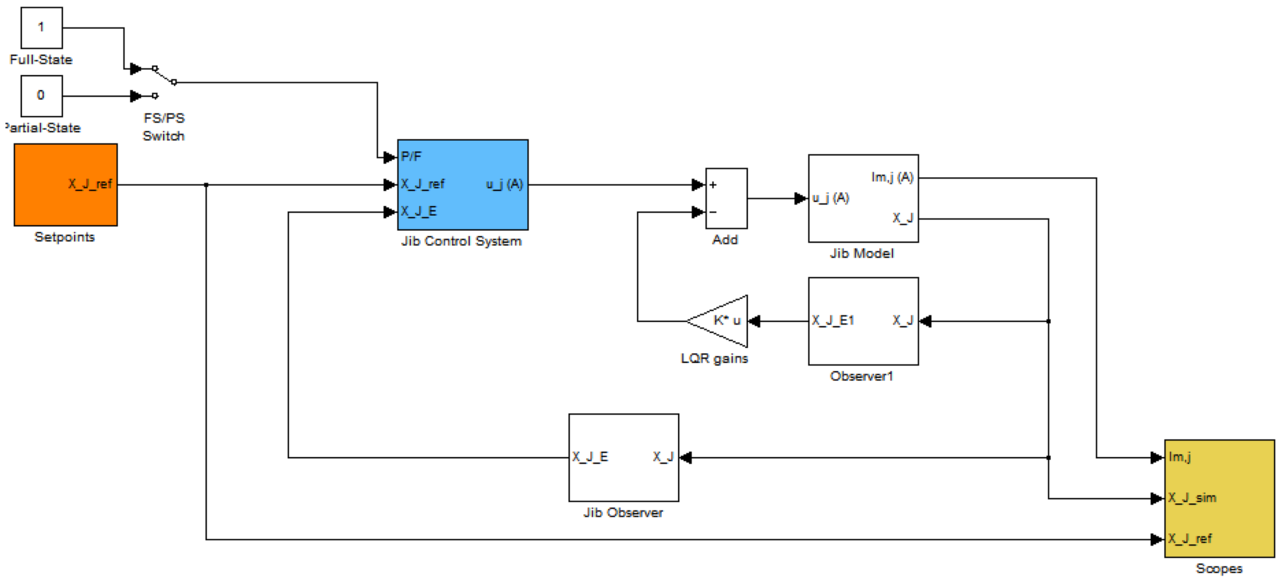

Figure 23: Simulink model of dual loop control scheme for the jib system

Chapter 6

Simulation and Experimental Results

6.1 Simulation Results

A number of simulations have been carried out on MATLAB/Simulink in context to find out the performance of our proposed scheme as compared to classical control schemes on jib system of 3DOF crane. The following section is dedicated to the simulation results. In next section, we have presented the validation of performance of proposed scheme as compared to classical control techniques on Quanser made 3DOF crane prototype. The experimental results are discussed in the next section.

6.1.1 Open Loop Response of the Jib System

Figure 23 and Figure 24 shows the open loop response of the trolley position and payload swing angle respectively.

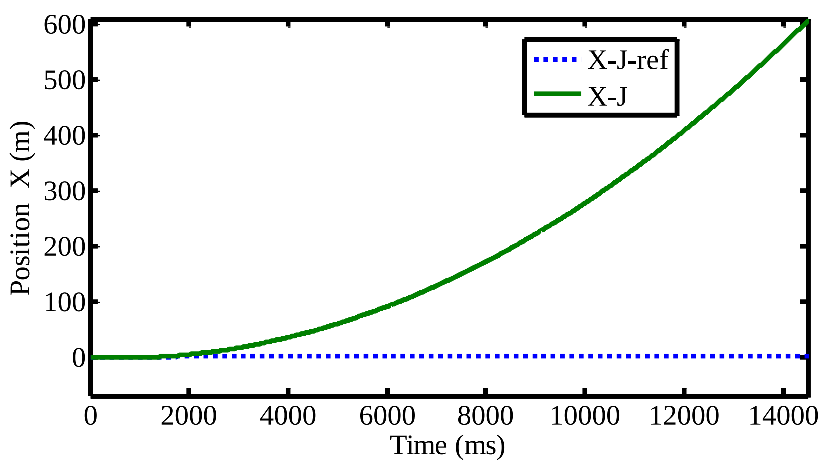

Figure 24: Open loop response of trolley position

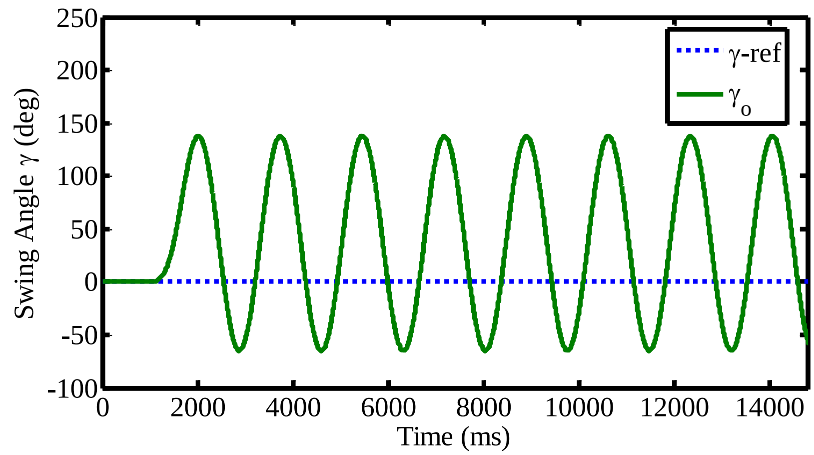

Figure 25: Open loop response of payload swing angle

This shows that maximum swing variations are 137.6 degrees in the clockwise direction and 64.92 degrees in the anti-clock wise direction. That is, beyond the limit of crane safe operation and the trolley is totally unstable. So, open loop system is not feasible for smooth operation of crane. There is a need of some control loop system which helps in smoothen the trolley trajectory by improving the payload vibration and trolley position simultaneously.

6.1.2 Performance of LQR tuned PID on the Jib System

Figure 25 and Figure 26 show the performance of PID tuned by LQR on the trolley position and payload swing angle respectively. It can be observed that the trolley position is stable as contrary to the open loop response of the system. Payload vibration improves by 94.41% in clockwise direction and 90.51% in a counterclockwise direction as compared to the open loop response of the system.

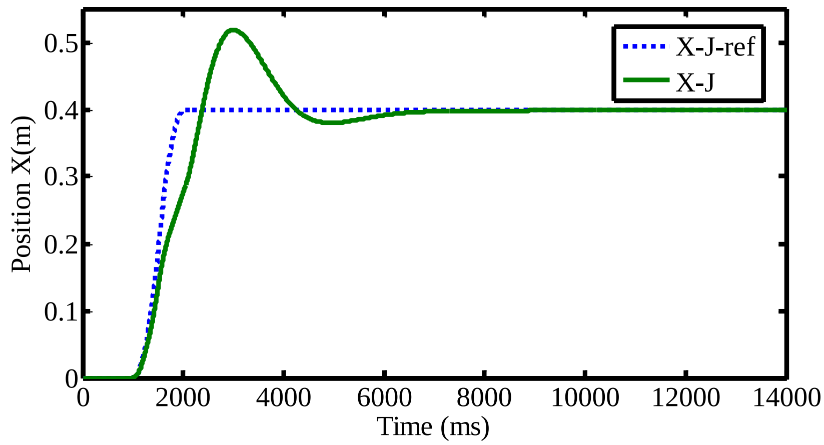

Figure 26: Response of trolley position with PID tuned by LQR

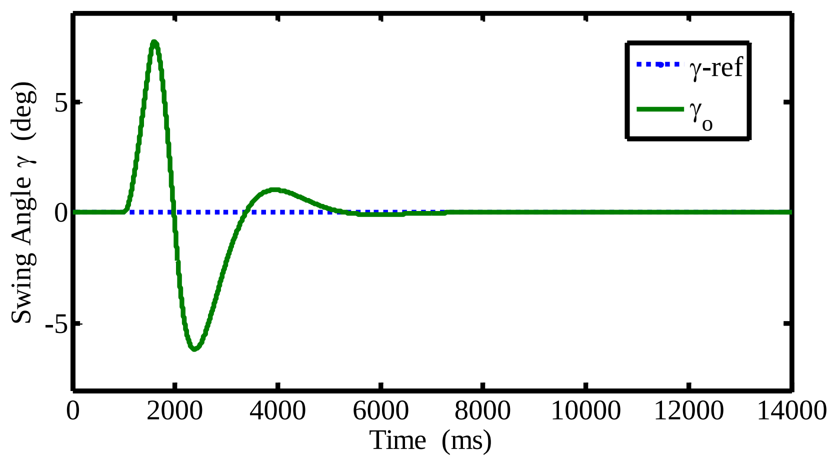

Figure 27: Response of payload swing with PID tuned by LQR

6.1.3 Performance of Pole Placement tuned PID on the Jib System

Figure 27 and Figure 28 show the performance of the PID tuned by pole placement on the trolley position and payload swing angle respectively. It can be observed that the trolley position is stable as contrary to the open loop response of the system. The payload vibration improves by 93.65% in clockwise direction and 87.13% in a counterclockwise direction as compared to the open loop response of the system.

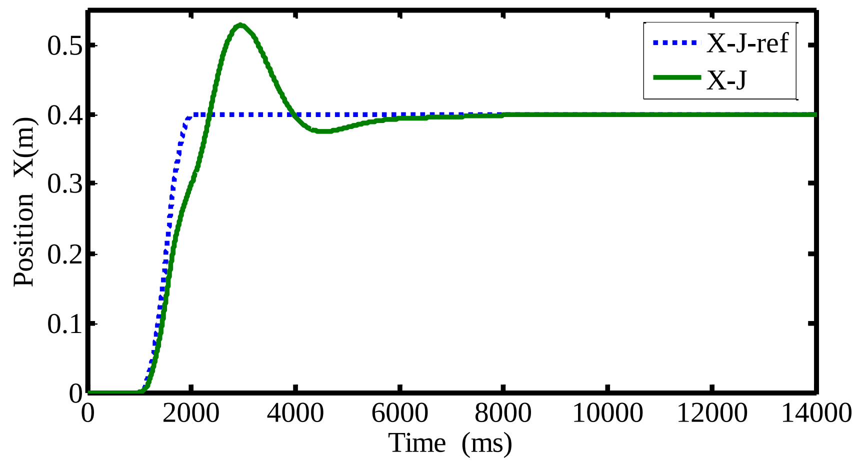

Figure 28: Response of trolley position with PID tuned by pole placement

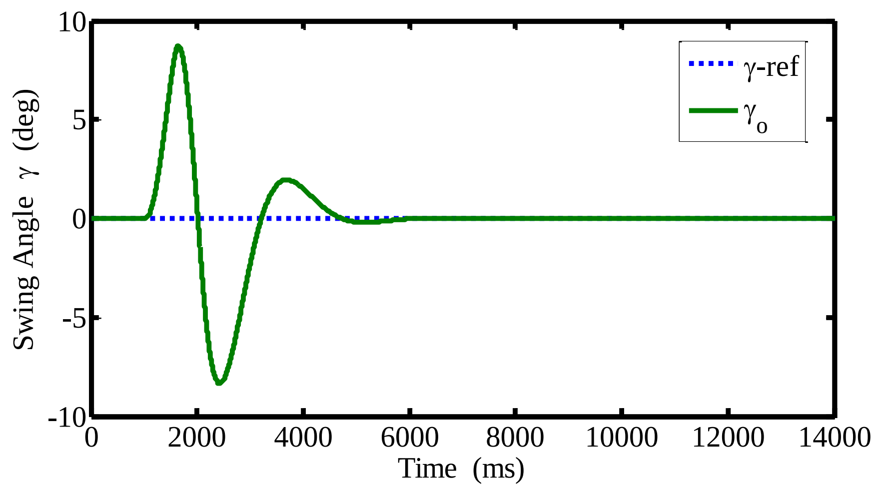

Figure 29: Response of payload swing with PID tuned by pole placement

6.1.4 Performance of Proposed Dual-Loop Control Scheme (DLCS) on Jib System

Figure 29 and Figure 30 show the performance of the proposed dual loop scheme on trolley position and payload swing angle respectively. It can be observed that the trolley position is stable as contrary to the open loop response of the system. Payload vibration improves by 94.70% in clockwise direction and 91.02% in a counterclockwise direction as compared to the open loop response of the system.

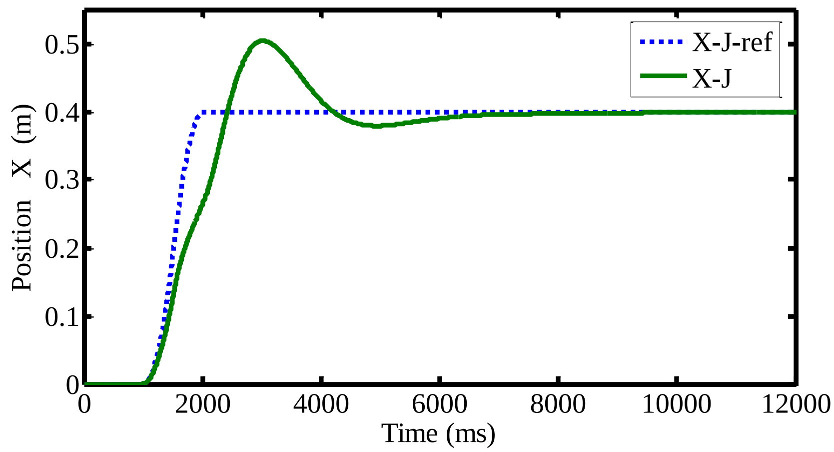

Figure 30: Response of trolley position with proposed dual-loop control scheme

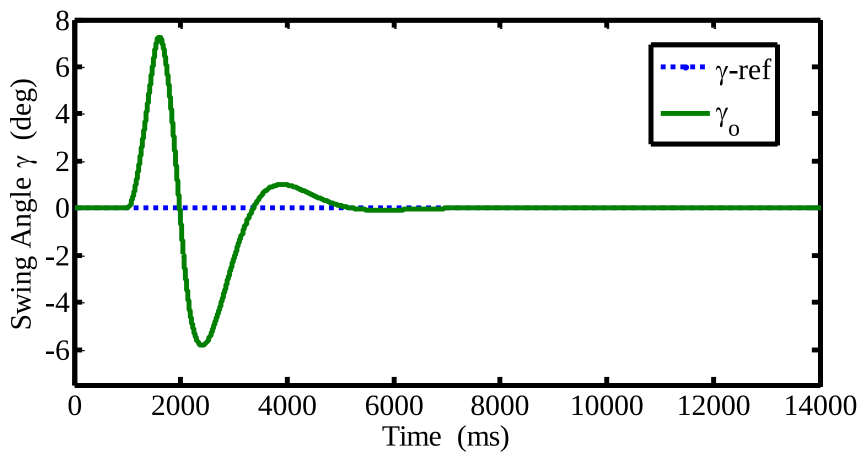

Figure 31: Response of payload swing with proposed dual-loop control scheme

6.1.1 Performance of all control techniques on the jib system

Figure 31 and Figure 32 compares the performance of all control techniques, namely PID tuned by LQR, PID tuned by pole placement and proposed dual-loop control scheme on the trolley position and payload swing angle respectively.

In Table 1, the performance of three control schemes is discussed on the basis of the payload swing angle. The results show that maximum payload vibration in anti-clock wise direction with

DLCS improves 5.32% and 30.20% as compared to PID tuned by LQR and PID tuned by pole placement respectively.

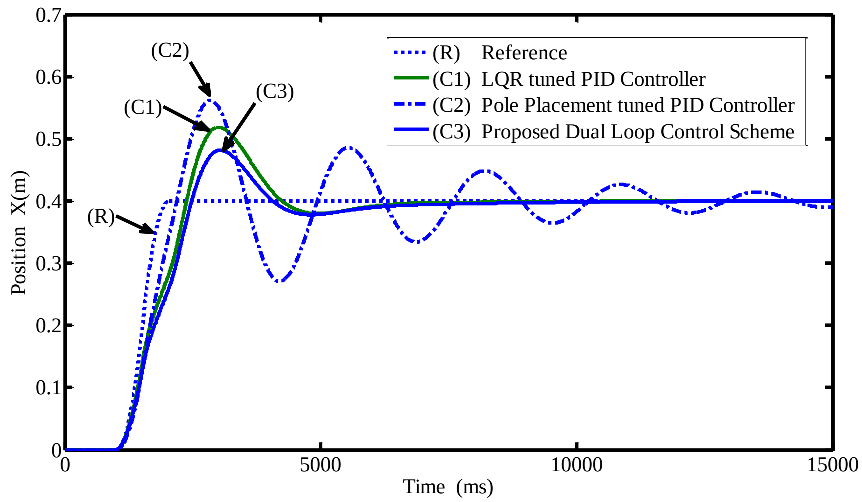

Figure 32: Response of trolley position with all applied control technique

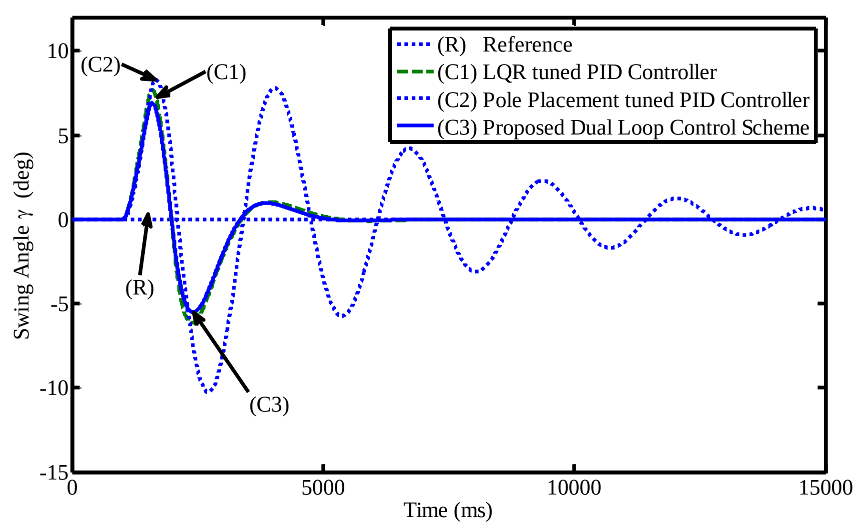

Figure 33: Response of payload swing with all applied control technique

The maximum payload vibration in a clockwise direction with DLCS improves 5.24% and 16.57% as compared to PID tuned by LQR and PID tuned by pole placement respectively. The settling time of the swing angle with DLCS improves 4.31% and 66.19% as compared to PID tuned by LQR and PID tuned by pole placement respectively.

The performance of all controllers on trolley position is summarized in table 2. An overshoot of trolley position with DLCS reduces 31.63% and 53.63% as compared to PID tuned by LQR and PID tuned by pole placement respectively.

Table 1: Performance comparison of all controllers on payload swing

S. No.	**Control Technique**	**Settling Time (Second)**	**Amplitude Diversion (Degree)**	
			Anti-Clock-wise	**Clockwise**
1.	PID Tuned By LQR	5.049	6.155	7.683
2.	PID Tuned by Pole Placement	14.29	8.349	8.726
3.	Proposed Dual Loop Scheme (DLCS)	4.831	5.827	7.28

Table 2: Performance comparison of all controllers on trolley position

S. No.	**Control Technique**	**Settling Time (Second)**	**Overshoot**
1.	PID Tuned By LQR	6.066	29.63
2.	PID Tuned by Pole Placement	14.34	44.02
3.	Proposed Dual Loop Scheme (DLCS)	6.448	20.41

6.2 Experimental Results

Figure 33 shows our actual hardware of 3DOF crane on which we have validated the performance of our control schemes. Results show that, by using our proposed control scheme performance measures like overshoot, steady state error and settling time along with payload vibration improves. It can be observed that actual system with manufacturer applied controller has some steady state error as shown in the Figure 34 and Figure 35 But our proposed controller caters this issue very effectively.

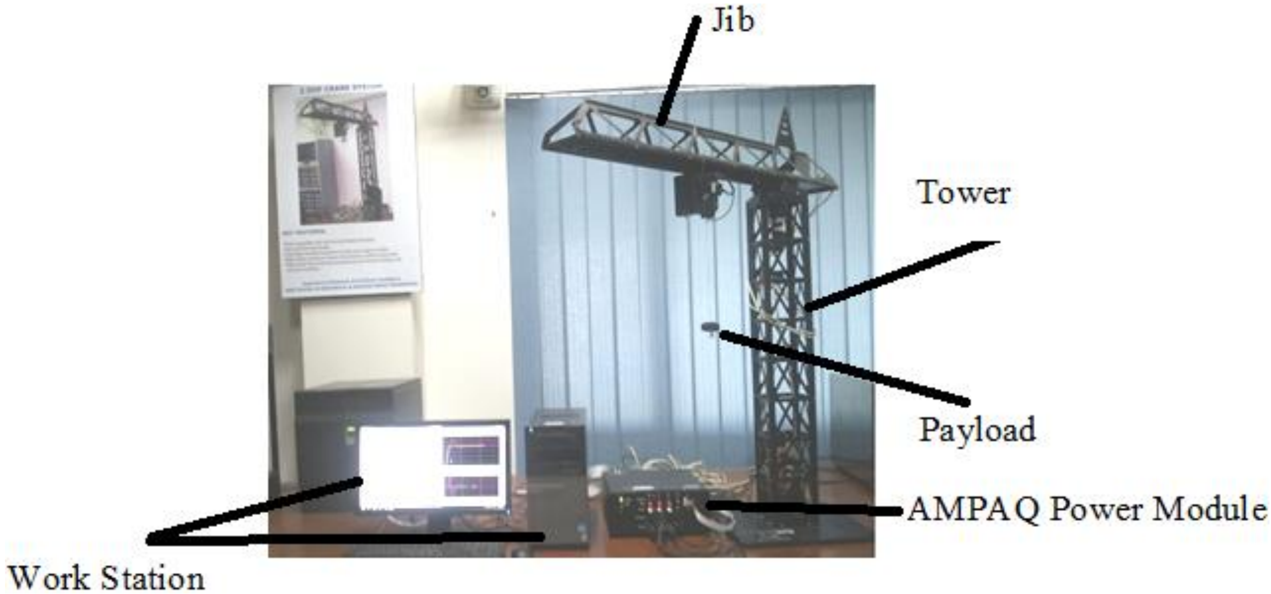

Figure 34: Hardware setup

The steady state error of trolley position using proposed scheme is improved by 90.78% and 91.66% as compared to PID tuned by LQR and PID tuned by pole placement respectively.

6.2.1 Performance of LQR tuned PID on the Jib System

Figure 34 and Figure 35 show the performance of PID tuned by LQR on trolley position and payload swing angle respectively. The trolley of the jib system settles in 1 seconds while payload oscillations settles in 2 seconds. Also, the trolley position has some steady state error. The payload vibration are 3.9 degrees in clock wise direction and 3.8 degrees in counter clock wise direction respectively.

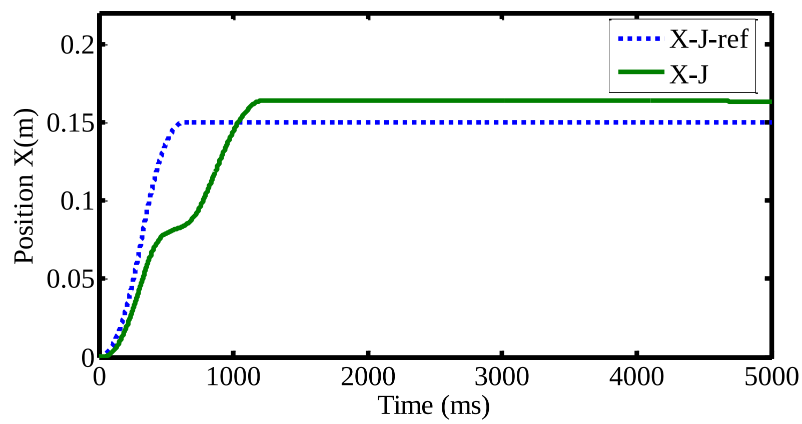

Figure 35: Response of trolley position with PID tuned by LQR

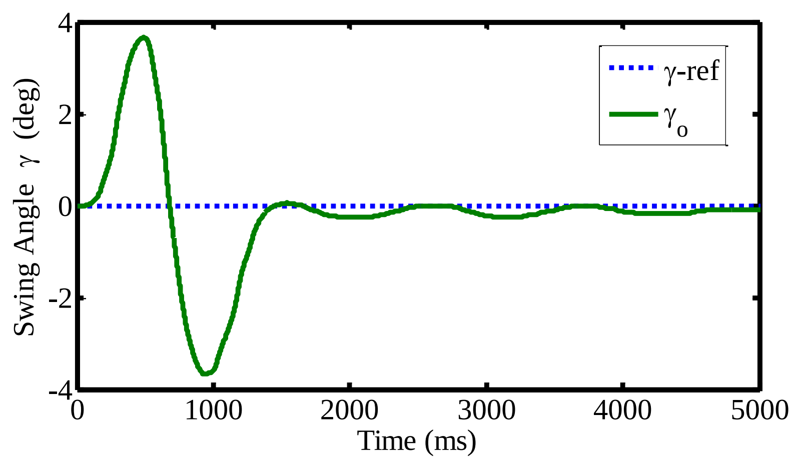

Figure 36: Response of payload swing with PID tuned by LQR

6.2.2 Performance of Pole Placement tuned PID on the Jib System

Figure 36 and Figure 37 show the performance of PID tuned by pole placement on trolley position and payload swing angle respectively.

The trolley of the jib system settles in 6 seconds while payload oscillations settles in 2 seconds. Also, the trolley position has some steady state error. The payload vibration are 2.4 degrees in clock wise direction and 1.8 degrees in counter clock wise direction respectively.

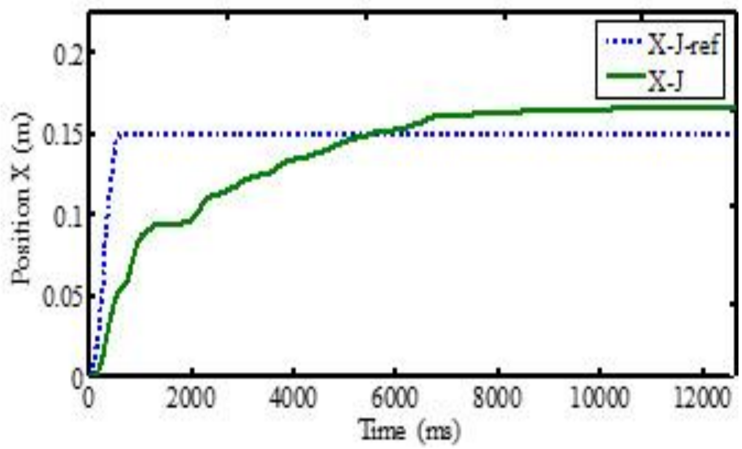

Figure 37: Response of trolley position with PID tuned by pole placement

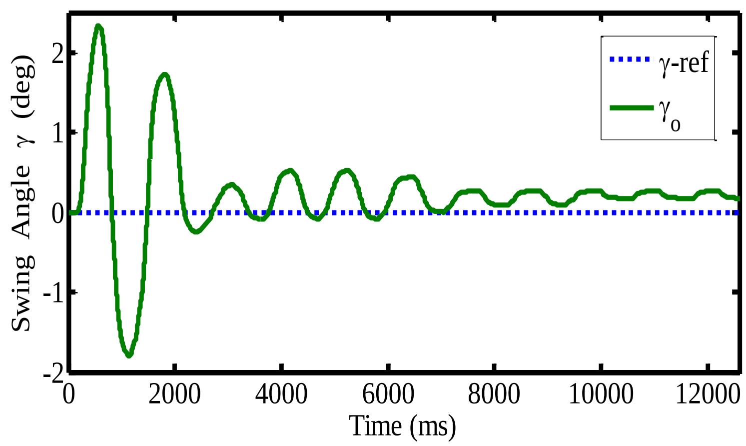

Figure 38: Response of payload swing with PID tuned by pole placement

6.2.3 Performance of Proposed Dual-Loop Control Scheme (DLCS) on the Jib system

Figure 38 and Figure 39 shows the performance of our proposed dual-loop control scheme on trolley position and payload swing angle respectively. The payload oscillations settles in 1 seconds while trolley of the jib system settles in 6.5 seconds. Also, the trolley position steady state error is improved effectively using proposed control scheme. The payload vibration are 2.5 degrees in clock wise direction and 3.5 degrees in counter clock wise direction respectively.

Table 3: Trolley position steady state error

S. No.	Control Scheme	Steady State Error
1.	LQR tuned PID Controller	0.0141
2.	Pole Placement tuned PID Controller	0.0156
3.	Proposed Dual Loop Control Scheme	0.0013

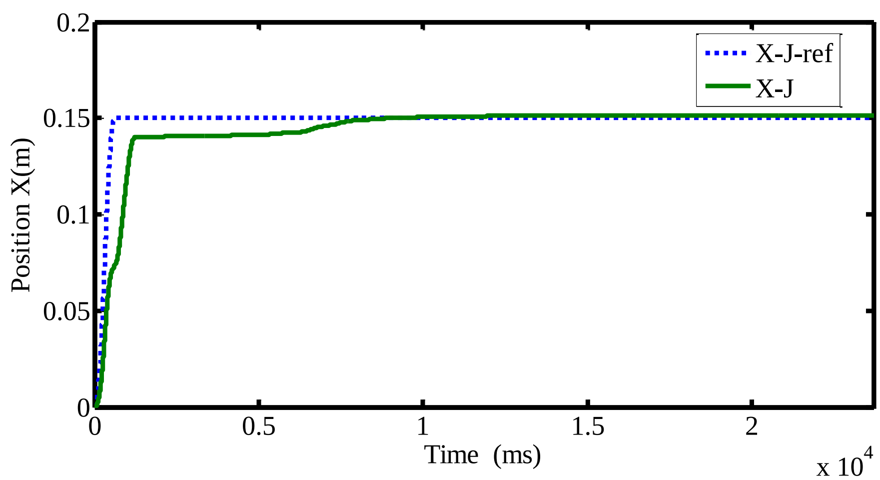

Figure 39: Response of trolley position with proposed dual loop control scheme

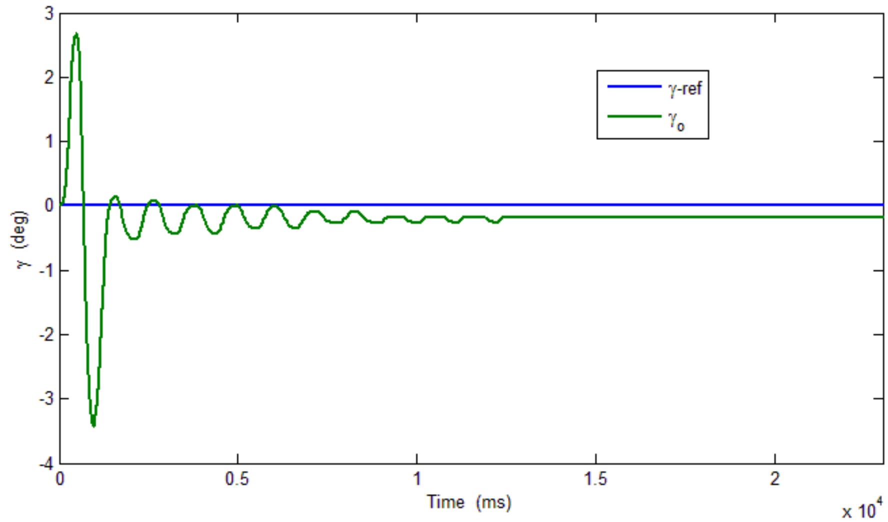

Figure 40: Response of payload swing with proposed dual loop control scheme

6.3 System Limitations and Risks

A number of limitations have been observed in the control of jib trolley of Quanser made 3DOF crane hardware in the loop. Following points summarizes limitations of Quanser made 3DOF crane prototype.

- There are only two states of the system, namely position and swing angle, which are directly accessible. In other words, 2nd derivative of position and swing angle are not directly measurable.
- A number of factors i.e. gravitational energy, potential energy and different resistive forces which affects the operation of crane are neglected during the modeling of the crane.
- A plane or smooth place is required for the placement of 3DOF crane.
- In the modeling of the jib system it is assumed that payload is subtended at certain angle, but in actual this angle is variable during operation of the crane.
- Sampling of the system should be in some specific range. More sampling time takes much energy and less sampling time results jerks in the trajectory of the trolley movement.

- A proper maintenance of the system is required otherwise dynamics of the system like friction varies up to unacceptable level.
- It is advised, avoid to check the open loop response of the system. It may damage the mechanical structure of the crane permanently.

Chapter 7

Conclusion and Future Recommendations

To control the trolley position and payload swing angle of the jib system of 3DOF crane, classical control techniques suffer from several shortcomings such as an overshoot, steady state error and settling time. To overcome these shortcomings alternative control scheme named as dual-loop control scheme (DLCS) has been proposed, implemented and investigated in this research work and a comparison with the classical PID control techniques has been carried out. The dual-loop control is actually a hybrid of classical PID and advance full state feedback control schemes.

The simulation and experimental results indicate that overshoot of trolley position with DLCS reduces 31.63% and 53.63% as compared to PID tuned by LQR and PID tuned by pole placement respectively. The maximum payload vibration in anti-clock wise direction with DLCS improves 5.32% and 30.20% as compared to PID tuned by LQR and PID tuned by pole placement respectively. The maximum payload vibration in a clockwise direction with DLCS improves 5.24% and 16.57% as compared to PID tuned by LQR and PID tuned by pole placement respectively. Settling time of the swing angle with DLCS improves 4.31% and 66.19% as compared to PID tuned by LQR and PID tuned by pole placement respectively. The steady state error of trolley position using DLCS is improved by 90.78% and 91.66% as compared to PID tuned by LQR and PID tuned by pole placement method respectively. In other words, our proposed scheme DLCS provides smooth trolley trajectory by improving the payload swing angle, overshoot, settling time and steady state error.

In the context of our future work, we have suggested the following recommendations:

- In this research work, we have developed a dual loop control scheme (DLCS) by a combination of PID and full state feedback. Here, LQR and pole placement techniques are used for tuning the PID. It is also possible to tune the PID by Fuzzy logic controller (FLC), Neuro fuzzy or any other technique

- Here hardware has also some limitations like 2nd derivatives of the output, i.e. velocity and rate of swing angle, are measured by estimation. There is no direct way to sense the 2nd derivatives of outputs. So, if sensors are placed to find the actual time varying values or 2nd derivatives of output, then applied controllers will be more effective.
- We have investigated the performance of our controllers on linear system. Although the system is nonlinear and linearized by Lagrange technique. Here, we have neglected kinetic energies, potential energies and some other dynamic factors for modeling of the system. So, it is also possible to investigate the performance of controllers on the actual nonlinear system.
- It is also possible to check the performance of controllers by applying noise or disturbance like Gaussian noise to the plant.
- A number of other control techniques like neuro-fuzzy and H- infinity are not applied to this hardware till yet.
- In this research work we have supposed that payload is fixed on specific height and at specific angle. So, it is also possible to test the effectiveness of controllers on the jib system by varying the rope length or payload angle.

References

[1] C.-C. Cheng and C.-Y. Chen, "Controller design for an overhead crane system with uncretainty," *Control Engineering Practice,* vol. 4, pp. 645-653, 1996.

[2] A. A. Al-Mousa, "Control of Rotary Cranes Using Fuzzy Logic and Time-Delayed Position Feedback Control," Virginia Polytechnic Institute and State University, 2000.

[3] J. Szpytko, J. Smoczek, and D. Lambskin, "ADAPTATIVE CONTROL SYSTEM OF OVERHEAD CRANE'S MOVEMENT MECHANISMES," presented at the International Carpathian Control Conference ICCC' 2002, MALENOVICE ,CZECH REPUBLIC, 2002.

[4] A. Benhidjeb and G. Gissinger, "Fuzzy control of an overhead crane performance comparison with classic control," *Control Engineering Practice,* vol. 3, pp. 1687-1696, 1995.

[5] S.-C. Kang, H.-L. Chi, and E. Miranda, "Three-dimensional simulation and visualization of crane assisted construction erection processes," *Journal of Computing in Civil Engineering,* vol. 23, pp. 363-371, 2009.

[6] A. CARRIER, E. Adhami, A. Stephens, and I. Murdoch, "Introducing a flexible manufacturing system," *THE INTERNATIONAL JOURNAL OF PRODUCTION RESEARCH,* vol. 22, pp. 907-916, 1984.

[7] J. Jafari, M. Ghazal, and M. Nazemizadeh, "A LQR Optimal Method to Control the Position of an Overhead Crane," *International Journal of Robotics and Automation (IJRA),* vol. 3, pp. 252-258, 2014.

[8] H.-H. Lee and S.-K. Cho, "A new fuzzy-logic anti-swing control for industrial three-dimensional overhead cranes," in *IEEE International Conference on Robotics and Automation, Proceedings 2001 ICRA.* , 2001, pp. 2956-2961.

[9] J. Abdullah, R. Ruslee, and J. Jalani, "Performance Comparison between LQR and FLC for Automatic 3 DOF Crane Systems," *International Journal of Control and Automation,* vol. 4, pp. 163-178, 2011.

[10] J. Jalani, "Anti-Swing Control Strategy for Automatic 3 DOF Crane System Using FLC," 2006.

[11] Y. Liang and K. Koh, "Concise anti-swing approach for fuzzy crane control," *Electronics Letters*, vol. 33, pp. 167-168, 1997.

[12] Y. Fang, W. Dixon, D. Dawson, and E. Zergeroglu, "Nonlinear coupling control laws for a 3-DOF overhead crane system," in *Decision and Control, 2001. Proceedings of the 40th IEEE Conference on*, 2001, pp. 3766-3771.

[13] S. Skogestad, "Simple analytic rules for model reduction and PID controller tuning," *Journal of process control*, vol. 13, pp. 291-309, 2003.

[14] A. Shapira, G. Lucko, and C. J. Schexnayder, "Cranes for building construction projects," *Journal of Construction Engineering and Management*, vol. 133, pp. 690-700, 2007.

[15] D. Lyddon, "Workplace Organization in the British Car Industry. A Critique of Jonathan Zeitlin," in *History Workshop*, 1983, pp. 131-140.

[16] B. Arendarski, W. Termath, and P. Mecking, "Maintenance of complex machines in electric power systems using virtual reality techniques," in *Electrical Insulation, 2008. ISEI 2008. Conference Record of the 2008 IEEE International Symposium on*, 2008, pp. 483-487.

[17] P. Cowling, "A flexible decision support system for steel hot rolling mill scheduling," *Computers & Industrial Engineering*, vol. 45, pp. 307-321, 2003.

[18] L. Black Jr Robert, "Unitary blowing and suction traveling cleaner for textile mills," ed: Google Patents, 1967.

[19] M. Barr, "Pulse width modulation," *Embedded Systems Programming*, vol. 14, pp. 103-104, 2001.

[20] D. Antic, Z. Jovanovic, S. Peric, S. Nikolic, M. Milojkovic, and M. Milosevic, "Anti-swing fuzzy controller applied in a 3D crane system," *Engineering, Technology & Applied Science Research*, vol. 2, pp. pp. 196-200, 2012.

[21] M. Jamil, A. A. Janjua, I. Rafique, S. I. Butt, Y. Ayaz, and S. O. Gilani, "Optimal Control based Intelligent Controller for Active Suspension System," *Life Science Journal*, vol. 10, 2013.

[22] M. J. Muhammad Faisal, Umair Iqbal and Yasar Ayaz, "Selection of Suitable Control Techniques for Payload Anti-Swing and Trolley Position Problems of 3DOF Crane," presented at the 1st Applied Mechanical Engineering Conference AMEC-ETEX 2014, Lahore, Pakistan, 2014.

[23] Y. J. Hua and Y. K. Shing, "Adaptive coupling control for overhead crane systems," in *Industrial Electronics Society, 2005. IECON 2005. 31st Annual Conference of IEEE*, 2005, p. 6 pp.

[24] H. Chen, B. Gao, and X. Zhang, "Dynamical modelling and nonlinear control of a 3d crane," in *Control and Automation, 2005. ICCA'05. International Conference on*, 2005, pp. 1085-1090.

[25] E. M. Abdel-Rahman, A. H. Nayfeh, and Z. N. Masoud, "Dynamics and control of cranes: A review," *Journal of Vibration and Control,* vol. 9, pp. 863-908, 2003.

[26] J. Huang, X. Xie, and Z. Liang, "Control of bridge cranes with distributed-mass payload dynamics," 2014.

[27] A. Hasanul Basher, "Swing-free transport using variable structure model reference control," in *SoutheastCon 2001. Proceedings. IEEE*, 2001, pp. 85-92.

[28] B. Vikramaditya and R. Rajamani, "Nonlinear control of a trolley crane system," in *American Control Conference, 2000. Proceedings of the 2000*, 2000, pp. 1032-1036.

[29] G. Corriga, A. Giua, and G. Usai, "An implicit gain-scheduling controller for cranes," *Control Systems Technology, IEEE Transactions on,* vol. 6, pp. 15-20, 1998.

[30] J. Yu, F. Lewis, and T. Huang, "Nonlinear feedback control of a gantry crane," in *Proceedings of the American Control Conference*, 1995, pp. 4310-4315.

[31] J. Lew and B. Halder, "Experimental study of anti-swing crane control for a varying load," in *PROCEEDINGS OF THE AMERICAN CONTROL CONFERENCE*, 2003, pp. 1434-1439.

[32] M. Jamil, S. Sharkh, M. Nasir Javid, and V. Nagendra, "Active control of vibrations of a tall structure excited by external forces," in *Proceedings of International Bhurban Conference on Appllied Science and Technology*, Pakistan, 2009, pp. 187-191.

[33] X. Zhang, Y. Fang, and N. Sun, "Minimum-time trajectory planning for underactuated overhead crane systems with state and control constraints," *IEEE TRANSACTIONS ON INDUSTRIAL Electronics Letters,* vol. 61, pp. 6915-6925, 2014.

[34] F. Panuncio, W. Yu, and X. Li, "Stable neural PID anti-swing control for an overhead crane," in *2013 IEEE International Symposium on Intelligent Control (ISIC)*, 2013, pp. 53-58.

[35] Z. Jovanović, D. Antić, Z. Stajić, M. Milošević, S. Nikolić, and S. Perić, "Genetic algorithms applied in parameters determination of the 3D crane model," *Facta universitatis-series: Automatic Control and Robotics,* vol. 10, pp. 19-27, 2011.

[36] A. Shebel, S. Maazouz, Z. Mohammed Abu, A. Mohammad, and R. Ayman Al, "Design of fuzzy PD-controlled overhead crane system with anti-swing compensation," *Journal of Engineering and Computer Innovations,* pp. 755-762, 2011.

[37] C.-Y. Chang and K.-H. Chiang, "The nonlinear 3-D crane control with an intelligent operating method," presented at the SICE Annual Conference 2008, The University Electro-Communications, 2008.

[38] J. M. M. Defoort, T. Murakami, "Integral sliding mode anti sway control of an underactuated overhead crane system," presented at the Mecatronics-REM Paris, 2012.

[39] H.-H. Lee, "A new motion-planning scheme for overhead cranes with high-speed hoisting," *Journal of Dynamic Systems, Measurement, and Control,* vol. 126, pp. 359-364, 2004.

[40] X. W. L. Y. W. Li and S. Shibin, "Anti-swing Control of the Crane System Based on Input Shaping Technique," *Computer & Digital Engineering,* vol. 2, 2011.

[41] L. Yanyang, X. Wei, and W. Li, "Anti-swing control of the crane system based on input shaping technique," in *2011 Chinese Control and Decision Conference (CCDC),* 2011, pp. 2788-2791.

[42] A. Kaneshige, Y. Kawasaki, S. Ueki, T. Miyoshi, and K. Terashima, "A design of the tele-operation control system for liquid container transfer by an overhead traveling crane," in *2014 11th International Conference on Remote Engineering and Virtual Instrumentation (REV),* 2014, pp. 29-30.

[43] J. Mendez, L. Acosta, L. Moreno, A. Hamilton, and G. Marichal, "Design of a neural network based self-tuning controller for an overhead crane," in *Control Applications, 1998. Proceedings of the 1998 IEEE International Conference on,* 1998, pp. 168-171.

[44] K. Nakazono, K. Ohnishi, H. Kinjo, and T. Yamamoto, "Vibration control of load for rotary crane system using neural network with GA-based training," *Artificial Life and Robotics,* vol. 13, pp. 98-101, 2008.

[45] R. Toxqui, W. Yu, and X. Li, "Anti-swing control for overhead crane with neural compensation," in *Neural Networks, 2006. IJCNN'06. International Joint Conference on,* 2006, pp. 4697-4703.

[46] Ş. Yildirim and I. b. Uzmay, "Neural network applications to vehicle’s vibration analysis," *Mechanism and Machine Theory,* vol. 38, pp. 27-41, 2003.

[47] J. Lin and W.-S. Chao, "Vibration suppression control of beam-cart system with piezoelectric transducers by decomposed parallel adaptive neuro-fuzzy control," *Journal of Vibration and Control,* vol. 15, pp. 1885-1906, 2009.

[48] K. Nakazono, K. Ohnisihi, and H. Kinjo, "Load swing suppression in jib crane systems using a genetic algorithm-trained neuro-controller," in *4th IEEE International Conference on Mechatronics, ICM 2007* 2007, pp. 1-4.

[49] H. Quan-yi, "Application of adaptive neuro-fuzzy inference system in anti-swing control to crane hook," *Hoisting and Conveying Machinery,* vol. 9, p. 006, 2007.

[50] C. Rekik, M. Djemel, and N. Derbel, "On the neuro-genetic approach for determining optimal control Of a rotary crane," in *Proceedings of 2003 IEEE Conference on Control Applications, 2003 CCA*, 2003, pp. 124-128.

[51] Quanser. *Quanser 3DOF Crane user manual*. Available: www.quanser.com/products/3dof_crane

[52] P. Kumar, O. Mehrotra, J. Mahto, and R. R. Mukherjee, "Modelling and Controller Design of Inverted Pendulum," in *National Conference on Communication, Measurement and Control*, 2012.

[53] D. P. Bertsekas, *Constrained optimization and Lagrange multiplier methods*: Academic press, 2014.

[54] H. Everett III, "Generalized Lagrange multiplier method for solving problems of optimum allocation of resources," *Operations research,* vol. 11, pp. 399-417, 1963.

[55] R. Hermann and A. J. Krener, "Nonlinear controllability and observability," *IEEE Transactions on automatic control,* vol. 22, pp. 728-740, 1977.

[56] J. C. Willems, "From time series to linear system—Part I. Finite dimensional linear time invariant systems," *Automatica,* vol. 22, pp. 561-580, 1986.

[57] D. Karanjkar, S. Chatterji, and A. Kumar, "Design and Implementation of a Linear Quadratic Regulator Based Maximum Power Point Tracker for Solar Photo-Voltaic System," *International Journal of Hybrid Information Technology,* vol. 7, pp. 167-182, 2014.

[58] P. Lancaster and L. Rodman, *Algebraic riccati equations*: Oxford University Press, 1995.

[59] D. Yue, Q.-L. Han, and C. Peng, "State feedback controller design of networked control systems," in *Control Applications, 2004. Proceedings of the 2004 IEEE International Conference on*, 2004, pp. 242-247.

[60] S. Suwankawin and S. Sangwongwanich, "A speed-sensorless IM drive with decoupling control and stability analysis of speed estimation," *Industrial Electronics, IEEE Transactions on,* vol. 49, pp. 444-455, 2002.

[61] T. Semba, T. Hirano, J. Hong, and L.-S. Fan, "Dual-stage servo controller for HDD using MEMS microactuator," *Magnetics, IEEE Transactions on,* vol. 35, pp. 2271-2273, 1999.

[62] H. Raut, A. Singh, and M. Patil, "Design of digital controller using pole placement method," presented at the International Conference on Control, Automation, Communication and Energy Conservation, 2009.

[63] S. Raghavan and J. K. Hedrick, "Observer design for a class of nonlinear systems," *International Journal of Control,* vol. 59, pp. 515-528, 1994.

[64] A. Kruczek, A. n. Stříbrský, K. i. Hyniová, and M. Hlinovský, "H-Infinity Controlled Actuators in Automotive Active Suspension System," in *ASME 2008 9th Biennial Conference on Engineering Systems Design and Analysis*, 2008, pp. 243-247.

[65] J. C. Doyle, K. Glover, P. P. Khargonekar, and B. A. Francis, "State-space solutions to standard H 2 and H∞ control problems," *Automatic Control, IEEE Transactions on,* vol. 34, pp. 831-847, 1989.

[66] Y. Lan and M. Fei, "Design of state-feedback controller by pole placement for a coupled set of inverted pendulums," presented at the 10th International Conference on Electronic Measurement & Instruments (ICEMI), 2011.

Appendix A:

Table 4: Nomenclature

S. No.	Symbol	Description
1	K_{t_j}	Torque constant of Jib motor
2	η_{m_j}	Efficiency of Jib motor
3	K_{g_j}	Gear ratio of Jib motor
4	η_{g_j}	Gearbox efficiency of Jib motor
5	r_{j_pulley}	Radius of trolley pulley from pivot to end of tooth
6	$m_{trolley}$	Mass of the trolley
7	J_{E_ψ}	Equivalent moment of inertia of Jib motor
8	l_{h_p}	Perpendicular distance of payload from Jib arm
9	g_{griv}	Acceleration constant of gravity
10	$m_{payload}$	Mass of payload
11	A_J	System state matrix
12	B_J	Input matrix
13	C_J	Output matrix
14	D_J	Direct transmission

Configure 3 DOF crane

```
% CONFIG_3D_CRANE
%
% Sets up the 3-DOF Crane Rev 4.0 Anti-Backlash system parameters and
% encoder calibration constants.
%
% Summary of system nomenclature:
% g             Gravitational acceleration                        (m/s^2)
% Kt_t          Motor Torque Constant: Tower                      (N.m/A)
% Kt_j          Motor Torque Constant: Jib                        (N.m/A)
% Kt_y          Motor Torque Constant: Trolley                    (N.m/A)
% eff_m_t       Tower Motor Efficiency
% eff_m_j       Jib Motor Efficiency
% eff_m_y       Trolley Motor Efficiency
% Kg_t          Motor Gear Ratio: Tower
% Kg_j          Motor Gear Ratio: Jib
% Kg_y          Motor Gear Ratio: Trolley
% eff_g_t       Gearbox Efficiency:
% eff_g_j       Gearbox Efficiency:
```

```
% eff_g_y       Gearbox Efficiency:
% J_theta       Equivalent Moment of Inertia about Tower Pivot      (kg.m^2)
% J_psi         Equivalent Moment of Inertia about Trolley Pivot    (kg.m^2)
% J_phi         Equivalent Moment of Inertia about Payload Pivot    (kg.m^2)
% J_alpha       Equivalent Moment of Inertia about Alpha Pendulum Pivot
(kg.m^2)
% J_gamma       Equivalent Moment of Inertia about Gamma Pendulum Pivot
(kg.m^2)
% lj            Max distance of trolley from pivot                  (m)
% lp            Vertical distance of payload from jib arm           (m)
% mp            Mass of the payload                                 (kg)
% m_trolley     Mass of trolley                                     (kg)
% r_y_reel      Radius of trolley reel mounted on trolley motor
%               (used to lift and release payload position)         (m)
% r_j_pulley    Radius of pulley wheel mount on jib motor
%               (used to move around the trolley)                   (m)
% Ka            AMPAQ gain                                          (A/V)
% K_CURR        AMPAQ current sensor calibration constnat           (A/V)
% K_ENC_THETA   Tower encoder calibration constant                  (rad/count)
% K_ENC_X       Trolley position encoder calibration constant       (m/count)
% K_ENC_Z       Payload elevation encoder calibration constant      (m/count)
% K_ENC_ALPHA   Gimble alpha deflection calibration constant        (rad/count)
% K_ENC_GAMMA   Gimble gamma deflection calibration constant       (rad/count)
%
% Copyright (C) 2010 Quanser Consulting Inc.
% Quanser Consulting Inc.
%
function [g, Kt_t, Kt_j, Kt_y, eff_m_t, eff_m_j, eff_m_y, Kg_t, Kg_j, Kg_y,
eff_g_t, eff_g_j, eff_g_y, J_theta, J_psi, J_phi, J_alpha, J_gamma, lj, lp, mp,
m_trolley, r_y_reel, r_j_pulley, Ka, K_CURR, K_ENC_THETA, K_ENC_X, K_ENC_Z,
K_ENC_ALPHA, K_ENC_GAMMA ] = config_3d_crane()
% Conversion factors
[ K_R2D, K_D2R, K_IN2M, K_M2IN, K_RDPS2RPM, K_RPM2RDPS, K_OZ2N, K_N2OZ, K_LBS2N,
K_N2LBS, K_G2MS, K_MS2G ] = calc_conversion_constants ();
% Gravitational constant (m/s^2)
g = 9.81;
% Pound to kg
% K_LBS2KG = K_LBS2N / g;
%
%% Tower Motor Parameters
% Motor current-torque constant (N.m/A)
Kt_t = 8.93;
% Motor efficiency
eff_m_t = 1.0;
% Motor Gearbox ratio
Kg_t = 100;
% Motor Gearbox efficiency
eff_g_t = 1.0;
% Motor Rotor Moment Of Inertia (kg.m^2)
Jm = 1.02e-6;
% Equivalent Rotor Moment Of Inertia at the harmonic drive shaft output (kg.m^2)
Jm_t = Kg_t^2 * Jm; % = 0.0102
%
%% Jib/Cart Motor Parameters
% Faulhaber 3042W 024C
% i.e. the motor that actuates the trolley movement
% Current-torque constant (N.m/A)
```

```
Kt_j = 5.608 * K_IN2M * K_OZ2N; % = 0.0396;
% Motor efficiency
eff_m_j = 0.79;
% Motor gearbox ratio
Kg_j = 3.7;
% Motor gearbox efficiency
eff_g_j = 0.95;
% Motor armature moment of inertia (kg.m^2)
Jm_j = 2.266e-4 * K_OZ2N / g * K_IN2M; % 1.6311e-007
%
%% Cart Linear Guide
% Pitch (m/rev)
Pt = 0.5 * K_IN2M;
%
%% Payload Motor Parameters
% Faulhaber 2342S 024CR
% Current-torque constant (N.m/A)
Kt_y = 0.0261;
% Motor efficiency
eff_m_y = 0.81;
% Motor gearbox (internal gear ratio)
Kg_y_i = 14;
% Motor to pulley gear ratio (external)
Kg_y_e = 2;
% Equivalent gear ratio from motor to pulley
Kg_y = Kg_y_i*Kg_y_e;
% Motor gearbox efficiency
eff_g_y = 1;
% Motor armature moment of inertia (kg.m^2)
Jm_y = 5.8/1000/100^2;
%
%% Trolley-related Mass and Length Parameters
% Payload mass (kg)
mp = 0.147; % mass of brass weight, black cover, and hook
% Maximum distance of payload from trolley (m)
lp = 34 * K_IN2M;
% Trolley mass (kg)
m_trolley = 0.60; % estimated using CAD
% Maximum position of trolley (m)
lj = 31.75 * K_IN2M;
%
%% Moment of Inertia about Tower Pivot
% Total mass of jib structure (kg)
m_j = 4.08;
% Total length of jib (m)
L_j = 1.205;
% Length of arm from tower pivot to end of trolley side (m)
L_j1 = 35.75 * K_IN2M;
% Length of jib from tower pivot to back end (m)
L_j2 = 12 * K_IN2M;
% Effective mass of front end (kg)
m_j1 = L_j1 * m_j / L_j;
% Effective mass of back end (kg)
m_j2 = L_j2 * m_j / L_j;
% Moment of inertia acting on tower pivot from jib (kg.m^2)
J_t_jib = 1 / 3 * m_j1 * L_j1^2 + 1/3 * m_j2 * L_j2^2;
%
```

```
%% Moment of Inertia of Jib
% Radius of jib motor pulley (m)
r_j_pulley = 0.560 / 2 * K_IN2M;
% Radius of jib motor pulley to outside rim (m)
r_j_pulley_od = 0.740 / 2 * K_IN2M;
% Mass of jib motor pulley (m)
m_j_pulley = 0.017; % **** MEASURE!!!
% Moment of inertia from pulley (kg.m^2)
J_j_pulley = 1/2 * m_j_pulley * r_j_pulley_od^2;
%
%% Moment of Inertia from Reel Mounted on Trolley Motor Shaft
% Radius of trolley reel (m)
r_y_reel = 1.125 / 2 * K_IN2M;
% Mass of trolley reel (kg)
m_y_reel = 0.030;
% Moment of inertia of trolley reel (kg.m^2)
J_y_reel = 1/2 * m_y_reel * r_y_reel^2;
%
%% Equivalent Moment of Inertia Calculations
% Tower equivalent moment of inertia (kg.m^2)
J_theta = Jm_t + J_t_jib;
% Jib equivalent moment of inertia (kg.m^2)
J_psi = Jm_j + J_j_pulley;
% Trolley equivalent moment of inertia (kg.m^2)
J_phi = Jm_y + J_y_reel;
% Gimble alpha deflection equivalent moment of inertia (kg.m^2)
J_alpha = 0;
% Gimble gamma deflection equivalent moment of inertia (kg.m^2)
J_gamma = 0;
%
%% AMPAQ Specifications
% Gain (A/V)
Ka = 0.5;
% Current sensor calibration consant (A/V)
K_CURR = -2.0;
%
%% Encoder Calibration Gains
% Tower encoder calibration constant (rad/count)
K_ENC_THETA = 2 * pi / (4 * 1024 ) / Kg_t;
% Trolley position encoder calibration constant (m/count)
K_ENC_X = - Pt / (4 * 1024 ) / Kg_j;
% Payload elevation encoder calibration constant (m/count)
K_ENC_Z = - 2 * pi * r_y_reel / (4 * 1024 ) / Kg_y;
% Gimble alpha deflection calibration constant (rad/count)
K_ENC_ALPHA = 2 * pi / (4 * 1024 );
% Gimble gamma deflection (calibration constant rad/count)
K_ENC_GAMMA = 2 * pi / (4 * 1024 );
```

Conversions

```
%% CALC_CONVERSION_CONSTANTS
%
% Calculates useful conversion factors w.r.t. units.
%
% Copyright (C) 2007 Quanser Consulting Inc.
```

```
% Quanser Consulting Inc.
%%
%
function [ K_R2D, K_D2R, K_IN2M, K_M2IN, K_RDPS2RPM, K_RPM2RDPS, K_OZ2N, K_N2OZ,
K_LBS2N, K_N2LBS, K_G2MS, K_MS2G ] = calc_conversion_constants ()
    % from radians to degrees
    K_R2D = 180 / pi;
    % from degrees to radians
    K_D2R = 1 / K_R2D;
    % from Inch to Meter
    K_IN2M = 0.0254;
    % from Meter to Inch
    K_M2IN = 1 / K_IN2M;
    % from rad/s to RPM
    K_RDPS2RPM = 60 / ( 2 * pi );
    % from RPM to rad/s
    K_RPM2RDPS = 1 / K_RDPS2RPM;
    % from oz-force to N
    K_OZ2N = 0.2780139;
    % from N to oz-force
    K_N2OZ = 1 / K_OZ2N;
    % Pound to Newton (N/lbs)
    K_LBS2N = 4.4482216;
    % Newton to Pound (lbs/N/)
    K_N2LBS = 1 / K_LBS2N;
    % from g to m/s^2
    K_G2MS = 9.81;
    % from m/s^2 to g
    K_MS2G = 1 / K_G2MS;
end
```

Call back Clear Setpoints

```
% On WinCon Controller Exit, set all the setpoint to zero, i.e. set the
% slider gains to 0.
% Tower Slider Gain Setpoint
set_param('q_3d_crane/Setpoints/Tower Setpoint (deg)','Gain','0');
% Trolley Slider Gain Setpoint
set_param('q_3d_crane/Setpoints/Trolley Setpoint (m)','Gain','0');
% Payload Slider Gain Setpoint
set_param('q_3d_crane/Setpoints/Payload Setpoint (m)','Gain','0');
```

Appendix B: Setup 3DOF crane

```
%SETUP_3D_CRANE
% Designs a state-feedback controller using the LQR technique for the
% Quanser 3D Crane Revision 4.0 device.
%
% Copyright (C) 2010 Quanser Consulting Inc.
% Quanser Consulting Inc.
%
% clear workspace
```

```
clear;
%
%% ##### LIMIT SWITCHES and SAFETY WATCHDOGS  #####
% Enable/Diable Limit Switches
LS_LIM_ENABLE = 1;
% LS_LIM_ENABLE = 0;
% Safety Watchdog: Trolley ON/OFF
X_LIM_ENABLE = 1;
% X_LIM_ENABLE = 0;
% Safety Limits on the trolley displacement (m)
X_MAX = 0.4;
X_MIN = - X_MAX;
% Safety Watchdog: Payload ON/OFF
Z_LIM_ENABLE = 1;
% Z_LIM_ENABLE = 0;
% Safety Limits on the payload displacement (m)
Z_MAX = 0.7;
Z_MIN = -0.05;
% Safety Watchdog: Alpha Pendulum Angle ON/OFF
ALPHA_LIM_ENABLE = 1;
% ALPHA_LIM_ENABLE = 0;
% Safety Limits on the pendulum angle (deg)
ALPHA_MAX = 25;
ALPHA_MIN = - ALPHA_MAX;
% Safety Watchdog: Gamma Pendulum Angle ON/OFF
GAMMA_LIM_ENABLE = 1;
% GAMMA_LIM_ENABLE = 0;
% Safety Limits on the pendulum angle (deg)
GAMMA_MAX = 25;            % pendulum angle maximum safety position (deg)
GAMMA_MIN = - GAMMA_MAX;   % pendulum angle minimum safety position (deg)
%
%% ##### HIGH-PASS FILTER PARAMETERS #####
% Tower HPF Parameters
wf_theta = 2 * pi * 50;
% Jib HPF Parameters
wf_x = 2 * pi * 50;
% Payload position HPF Parameters
wf_z = 2 * pi * 50;
% Alpha Gimble deflection HPF Parameters
wf_alpha = 2 * pi * 50;
% Gamma Gimble deflection HPF Parameters
wf_gamma = 2 * pi * 2.0;
% ##### END OF USER-DEFINED FILTER PARAMETERS #####
%
%% ##### BUILD OPEN-LOOP MODEL #####
% AMPAQ Maximum Output Current (A)
IMAX_AMP = 7;
% Digital-to-Analog Maximum Voltage (V); for Q4/Q8 cards set to 10
VMAX_DAC = 10;
% load 3D Crane model parameters and sensor calibration constants
[g, Kt_t, Kt_j, Kt_y, eff_m_t, eff_m_j, eff_m_y, Kg_t, Kg_j, Kg_y, eff_g_t,
eff_g_j, eff_g_y, J_theta, J_psi, J_phi, J_alpha, J_gamma, lj, lp, mp,
m_trolley, r_y_reel, r_j_pulley, Ka, K_CURR, K_ENC_THETA, K_ENC_X, K_ENC_Z,
K_ENC_ALPHA, K_ENC_GAMMA ] = config_3d_crane();
% state-space of the 3D Crane Tower subsystem.
CRANE_TOWER_ABCD_eqns;
A_T = A; B_T = B; C_T = C; D_T = D;
```

```
clear A B C D;
% state-space of the 3D Crane Jib subsystem.
B_psi = 0;
B_gamma = 0;
CRANE_JIB_ABCD_eqns;
% add an integrator to the Jib system
A_J = A; B_J = B; C_J = C; D_J = D;
A_J(5,1) = 1;
A_J(5,5) = 0;
B_J(5) = 0;
%
clear A B C D;
```

Controller Design

```
%% ##### USER_DEFINED CONTROL SYSTEM DESIGN #####
% Tower controller
Q_T = diag([2 1 0.25 0.25]);
R_T = 0.05;
K_T = lqr(A_T,B_T,Q_T,R_T);
%
% Jib controller
Q_J = diag([5 5 1 5 1]);
% Q_J = diag([75 5 5 15 5]);
Q_J = diag([5 5 1 5 1]);
R_J = 0.05;
K_J = lqr(A_J,B_J,Q_J,R_J);
%
% Payload position controller
% Percentage overshoot specification (%)
PO = 10;
% Peak time specification (s)
% tp = 0.05;
tp = 0.02;
% Zero location specifiation (rad/s)
p0 = 0.125;
% Calculate PIV gains
[ kp, kv, ki ] = d_payload_piv_controller( Kt_y, eff_m_y, Kg_y, eff_g_y, J_phi,
mp, r_y_reel, PO, tp, p0 );
%
%% ##### DEBOUNCE PARAMETERS #####
% Debounce is trigerred when the average of the last 'dbnc_samples' is
% greater than the threshold.
dbnc_threshold = 0.8;
% Number of samples in input signal used in average calculation.
dbnc_samples = 0.01 / 1e-3; % duration (s) dividied by sample time (Hz)
%
%% ##### CALIBRATION PARAMETERS #####
% Desired HOME positions after encoders have been reset
% Tower Home Setpoint (deg)
sp_home_tower = 155;
% Trolley Home Setpoint (m)
sp_home_trolley = 0.25;
% Payload Home Setpoint (deg)
sp_home_payload = -0.7;
```

```
%
% Calibration Threshold: abs of position & velocity error has to be
% less than these values
% Tower Calibration Position Threshold (rad)
calib_theta = 4.5*pi/180;
% Trolley Calibration Position Threshold (m)
calib_x = 2/100;
% Payload Calibration Position Threshold (m)
calib_z = 3/100;
% Tower Calibration Velocity Threshold (rad/s)
calib_theta_dot = 1/1000;
% Trolley Calibration Velocity Threshold (m/s)
calib_x_dot = 2/1000;
% Payload Calibration Velocity Threshold (m/s)
calib_z_dot = 5/1000;
% Position threshold that detects if tower is stuck at right limit
% If the tower is not close to setpoint and at zero velocity, then it is at
% the right limit switch.
calib_theta_r = 15.0*pi/180;
%
%% ##### DISPLAY #####
disp(' ');
disp('Tower Control Gain:');
disp( ['    K_T  = [' num2str(K_T,3) ' ]' ]);
disp(' ');
disp('Jib Control Gain:');
disp( ['    K_J  = [' num2str(K_J,3) ' ]' ]);
disp(' ');
disp('PIV Trolley Control gains:');
disp( ['    kp = ' num2str(kp,3) ' A/m']);
disp( ['    ki = ' num2str(ki,3)  ' A/m/s']);
disp( ['    kv = ' num2str(kv,3) ' A.s/m' ]);
```

Jib System Matrices

```
% Matlab equation file: "CRANE_JIB_ABCD_eqns.m"
% Open-Loop State-Space Matrices: A, B, C, and D
% for the Quanser 3D CRANE TROLLEY/PENDULUM MODEL Experiment.

A( 1, 1 ) = 0;
A( 1, 2 ) = 0;
A( 1, 3 ) = 1;
A( 1, 4 ) = 0;
A( 2, 1 ) = 0;
A( 2, 2 ) = 0;
A( 2, 3 ) = 0;
A( 2, 4 ) = 1;
A( 3, 1 ) = 0;
A( 3, 2 ) = -
r_j_pulley^2*mp^2*lp^2*g/(m_trolley*r_j_pulley^2*mp*lp^2+m_trolley*r_j_pulley^2*
J_gamma+mp*r_j_pulley^2*J_gamma+J_psi*Kg_j^2*mp*lp^2+J_gamma*Kg_j^2*J_psi);
A( 3, 3 ) = -
r_j_pulley^2*B_psi*(mp*lp^2+J_gamma)/(m_trolley*r_j_pulley^2*mp*lp^2+m_trolley*r
_j_pulley^2*J_gamma+mp*r_j_pulley^2*J_gamma+J_psi*Kg_j^2*mp*lp^2+J_gamma*Kg_j^2*
J_psi);
```

```
A( 3, 4 ) = -
r_j_pulley^2*mp*lp*B_gamma/(m_trolley*r_j_pulley^2*mp*lp^2+m_trolley*r_j_pulley^
2*J_gamma+mp*r_j_pulley^2*J_gamma+J_psi*Kg_j^2*mp*lp^2+J_gamma*Kg_j^2*J_psi);
A( 4, 1 ) = 0;
A( 4, 2 ) = -
mp*g*lp*(m_trolley*r_j_pulley^2+mp*r_j_pulley^2+J_psi*Kg_j^2)/(m_trolley*r_j_pul
ley^2*mp*lp^2+m_trolley*r_j_pulley^2*J_gamma+mp*r_j_pulley^2*J_gamma+J_psi*Kg_j^
2*mp*lp^2+J_gamma*Kg_j^2*J_psi);
A( 4, 3 ) = -
B_psi*r_j_pulley^2*mp*lp/(m_trolley*r_j_pulley^2*mp*lp^2+m_trolley*r_j_pulley^2*
J_gamma+mp*r_j_pulley^2*J_gamma+J_psi*Kg_j^2*mp*lp^2+J_gamma*Kg_j^2*J_psi);
A( 4, 4 ) = -
B_gamma*(m_trolley*r_j_pulley^2+mp*r_j_pulley^2+J_psi*Kg_j^2)/(m_trolley*r_j_pul
ley^2*mp*lp^2+m_trolley*r_j_pulley^2*J_gamma+mp*r_j_pulley^2*J_gamma+J_psi*Kg_j^
2*mp*lp^2+J_gamma*Kg_j^2*J_psi);

B( 1, 1 ) = 0;
B( 2, 1 ) = 0;
B( 3, 1 ) =
r_j_pulley*eff_g_j*Kg_j*eff_m_j*Kt_j*(mp*lp^2+J_gamma)/(m_trolley*r_j_pulley^2*m
p*lp^2+m_trolley*r_j_pulley^2*J_gamma+mp*r_j_pulley^2*J_gamma+J_psi*Kg_j^2*mp*lp
^2+J_gamma*Kg_j^2*J_psi);
B( 4, 1 ) =
eff_g_j*Kg_j*eff_m_j*Kt_j*r_j_pulley*mp*lp/(m_trolley*r_j_pulley^2*mp*lp^2+m_tro
lley*r_j_pulley^2*J_gamma+mp*r_j_pulley^2*J_gamma+J_psi*Kg_j^2*mp*lp^2+J_gamma*K
g_j^2*J_psi);

C( 1, 1 ) = 1;
C( 1, 2 ) = 0;
C( 1, 3 ) = 0;
C( 1, 4 ) = 0;
C( 2, 1 ) = 0;
C( 2, 2 ) = 1;
C( 2, 3 ) = 0;
C( 2, 4 ) = 0;

D( 1, 1 ) = 0;
D( 2, 1 ) = 0;
```

Controller Gains Calculations

```
%System matrices
A_J
B_J
C_J
D_J

%Check controllability and observability
crtb(A,B)
obsv(A,C)

%LQR Controller
Q=[5 0 0 0 0;
   0 5 0 0 0;
```

```
   0 0 1 0 0;
   0 0 0 5 0;
   0 0 0 0 1]
R=0.1
K=LQR(A,B,Q,R)

%PID tuning using Pole Placement
Ps=eig(I)   % system poles
Pd=[-1-i -1+i -3+10.1*i -3-10.1*i -2]
K=Place(A,B,P)

%Proposed Dual loop scheme
%Gains value K for state feedback part of proposed dual loop scheme
R=1
K=LQR(A,B,Q,R)

% Gains value L for observer
Pd=5*[-1-1i -1+i -3+10.1*i -3-10.1*i]
L=Place(A_J,B_J,Pd)
```